

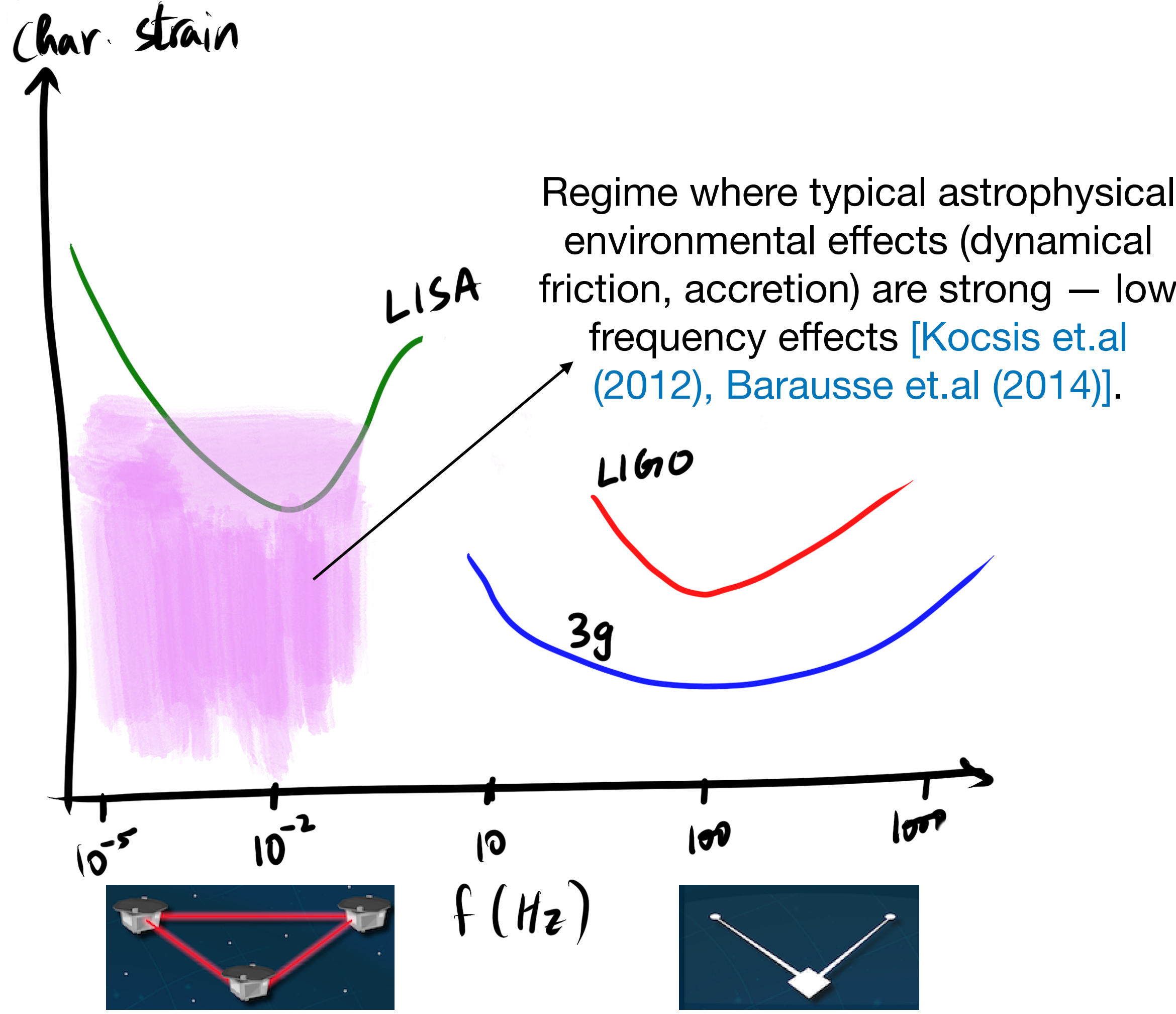
Probing astrophysical environments of stellar mass black hole binaries through the LISA stochastic signal

Rohit S. Chandramouli
SISSA (postdoc)

Collaborators: Ran Chen, Federico Pozzoli,
Riccardo Buscicchio, Enrico Barausse
BiCoQ conference [2507.00694, 2605.05537]



Early inspiral, low frequency regime of stellar mass black hole binaries: window into astrophysical environment



- Probing environmental effects with resolvable stellar-mass BBH (sBBH) in LISA:
 - Dynamical friction and accretion [Toubiana et.al (2021), Caputo et.al (2020)]
 - Third body effects [Sberna et.al (2022)]

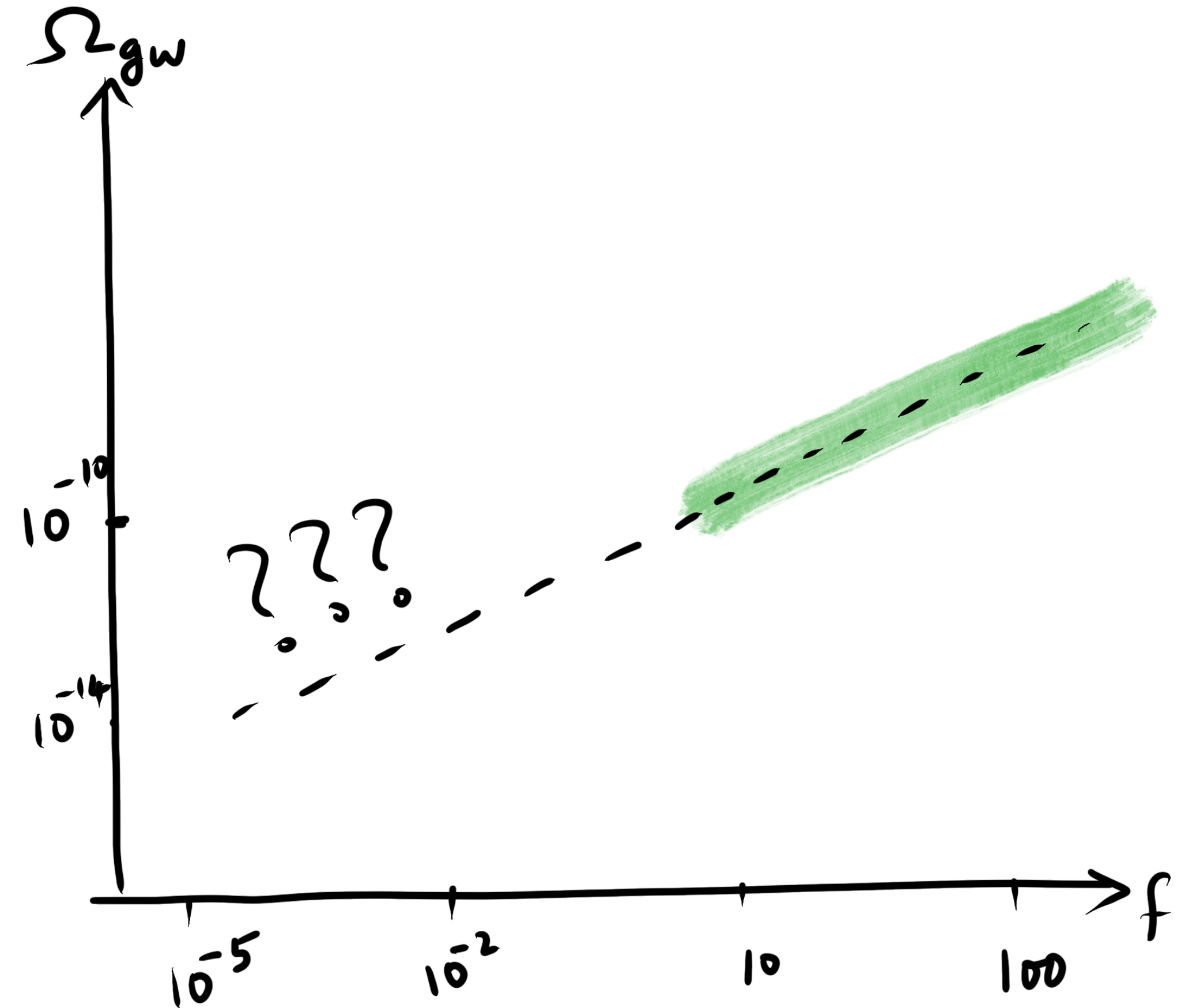
- **Can we probe environmental effects from unresolved sBBH in LISA through the resulting stochastic GW background (SGWB)?**

Primer on SGWB from vacuum sBBH

Astrophysical SGWB is just the sum of independent GW signals from unresolved population of sources.

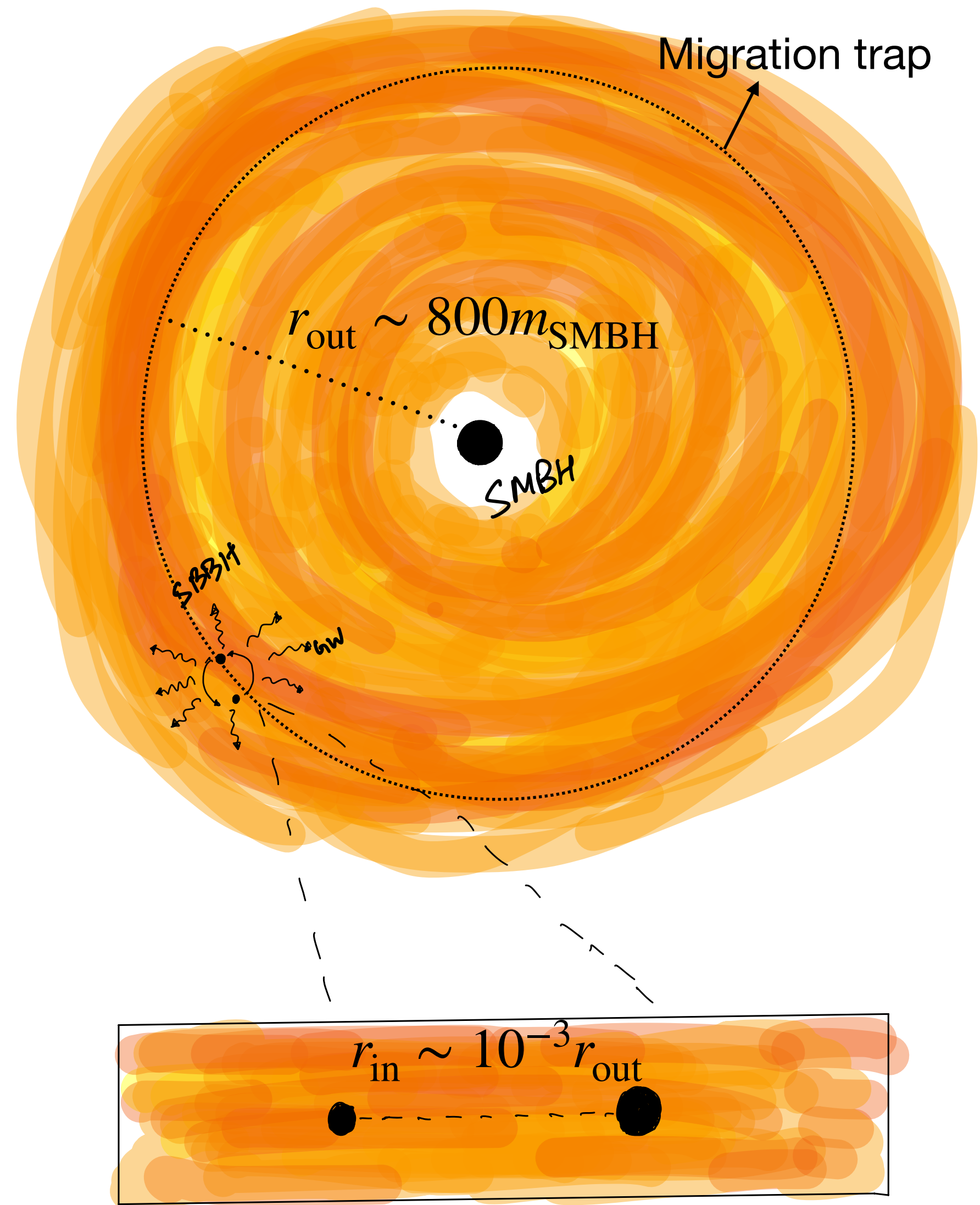
SGWB spectrum is characterized by the dimensionless, normalized GW energy density (per logarithmic frequency) $\Omega_{\text{GW}}(f)$

If sBBH were in vacuum, $\Omega_{\text{GW}}(f) = A_{\text{vac}} f^{2/3}$

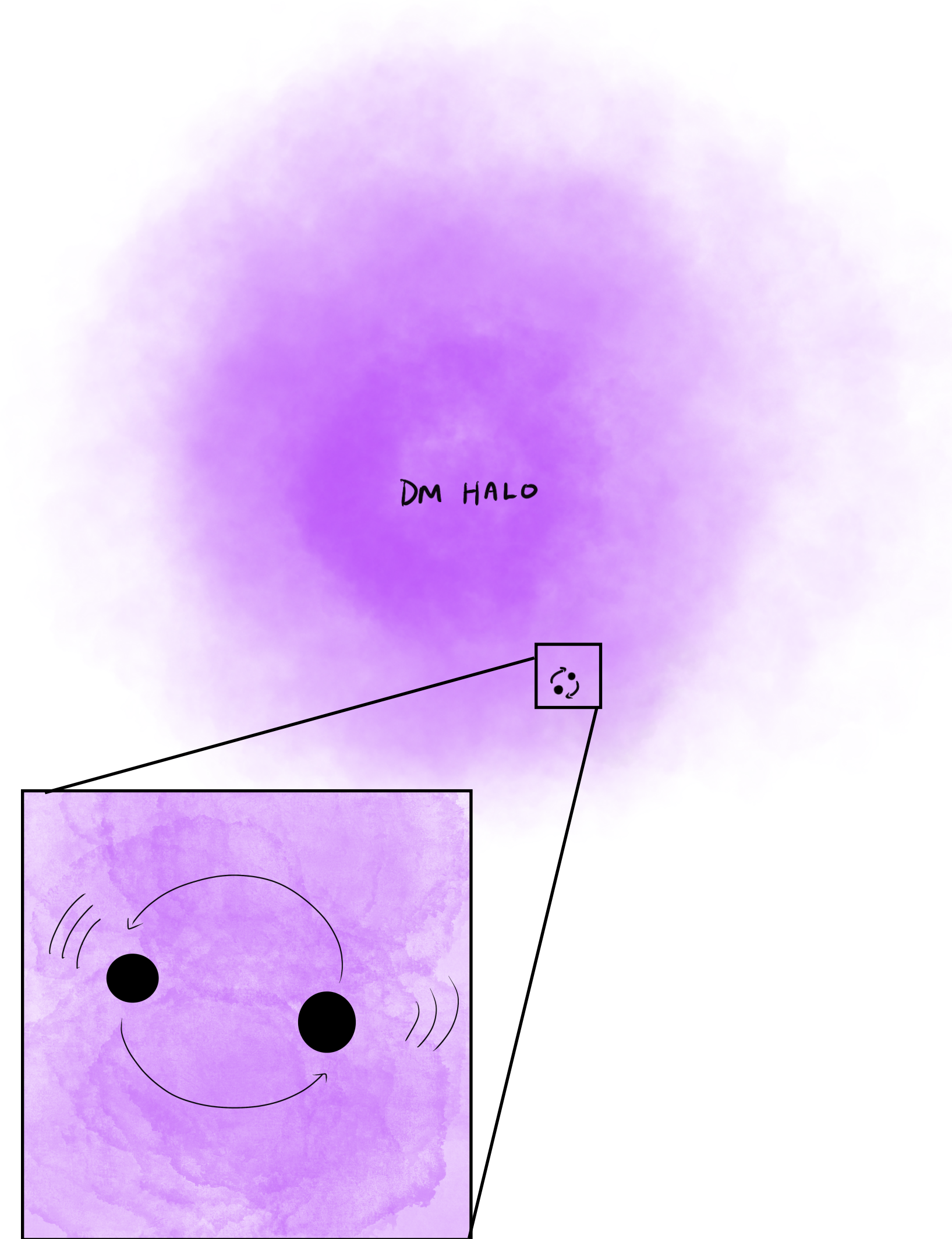


Primer on environmental effects

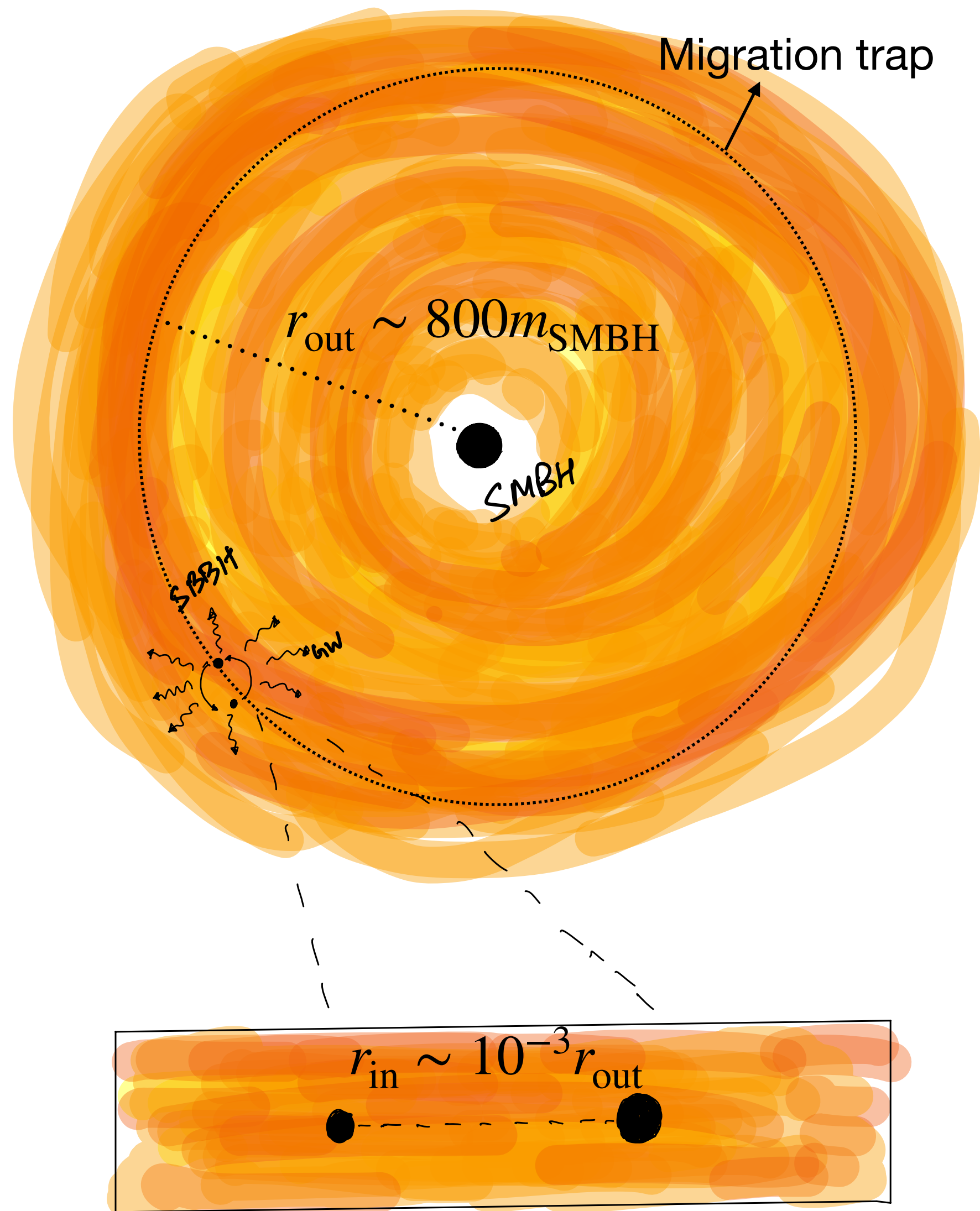
sBBH in AGN disk



sBBH in DM halo



Primer on environmental effects



Gas effects from the disc: [Yunes etal (2011), Kocsis etal (2012), Barausse etal (2014), Caputo etal (2020), Toubiana etal (2021)]

- **Dynamical friction:** Gravitational drag due to density wakes [-5.5PN].
- **Accretion:** Adiabatic change in masses of sBBH + hydrodynamic drag due to momentum exchange [-4PN]
- Third body effects:
 - Line of sight CoM acceleration / Doppler delay effect [-4PN*]
 - Shapiro time delay
 - Gravitational lensing, de Sitter precession, Kozai-Lidov oscillations, precessional resonances etc.

Effect of environmental effects on energy spectrum

Energy spectrum of binary in vacuum:

$$\left(\frac{dE_{\text{GW}}}{df_s}\right)_{\text{vac}} = \frac{\eta m^{5/3} \pi^{2/3}}{3f_s^{1/3}}$$

Energy spectrum of binary with (supersonic) dynamical friction effects:

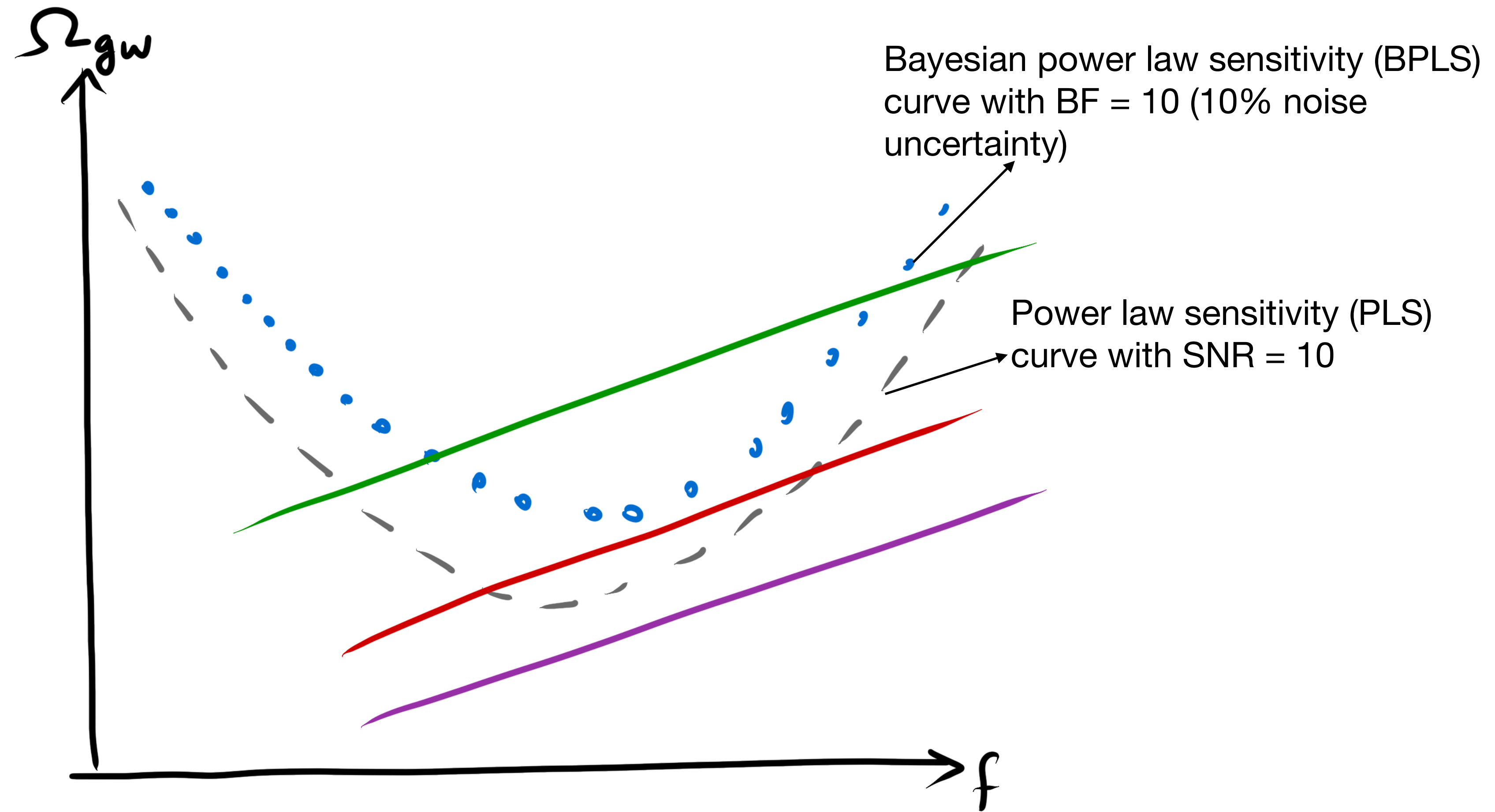
$$\left(\frac{dE_{\text{GW}}}{df_s}\right)_{\text{DF}} = \left(\frac{dE_{\text{GW}}}{df_s}\right)_{\text{vac}} \left\{ 1 + \frac{5\rho f_s^{-11/3}}{8\pi^{8/3}\eta^3 m^{14/3}} \times \left[m_1^3 \ln\left(\frac{f_1^*}{f_s}\right) + (m_1 \leftrightarrow m_2) \right] \right\}^{-1}, \quad \frac{f_{\text{turn}}}{(\ln[1\text{Hz}/f_{\text{turn}}])^{3/11}} \approx (1.69 \times 10^{-3}\text{Hz}) \left(\frac{m}{50M_{\odot}}\right)^{-5/11} \left(\frac{\rho}{10^{-10}\text{g cm}^{-3}}\right)^{3/11}$$

Energy spectrum of binary with (Eddington rate parametrized) accretion effects:

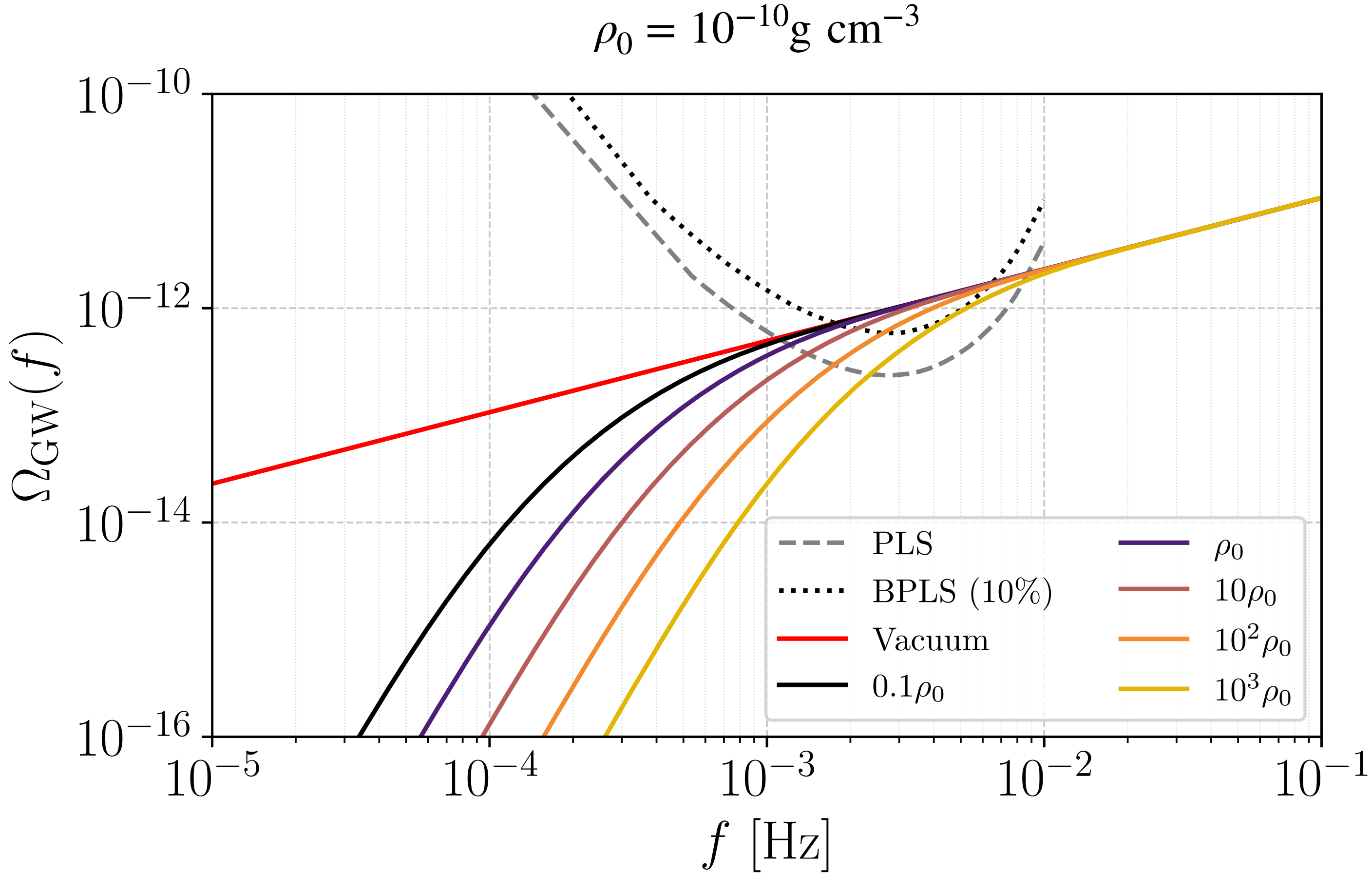
$$\left(\frac{dE_{\text{GW}}}{df_s}\right)_{\text{Acc}} = \left(\frac{dE_{\text{GW}}}{df_s}\right)_{\text{vac}} \left[1 + \frac{5(f_{\text{Edd}}/\tau)(5+3\xi)}{96\pi^{8/3}m_0^{5/3}\eta} f_s^{-8/3} \right]^{-1}, \quad f_{\text{turn}} \approx 10^{-4}\text{Hz} \left(\frac{f_{\text{edd}}}{1}\right)^{3/8} \left(\frac{m}{50M_{\odot}}\right)^{-5/8} \left(\frac{5+3\xi}{8}\right)^{3/8} \left(\frac{\tau}{4.5 \times 10^7\text{yr}}\right)^{-3/8}$$

Is your stochastic signal detectable?

[Pozzoli, Gair, Buscicchio, Speri, PRD (2025)]

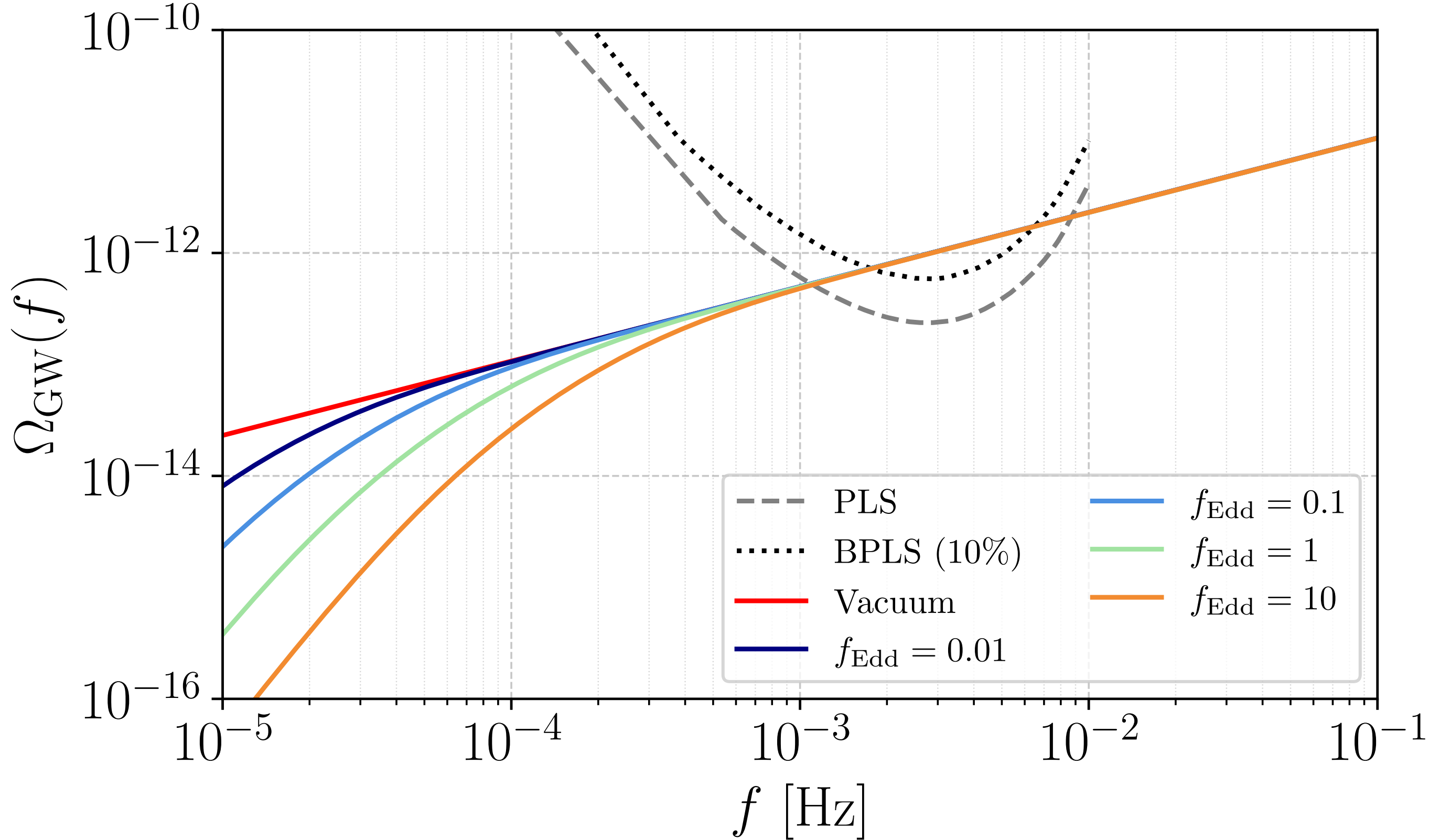


SGWB of sBBH with dynamical friction effects in LISA: qualitative detectability



- Vacuum case is above both PLS and BPLS curves in a significant part of the LISA band → vacuum signal potentially detectable
- Dynamical friction effects are potentially detectable due to turning point in sensitive part of LISA band

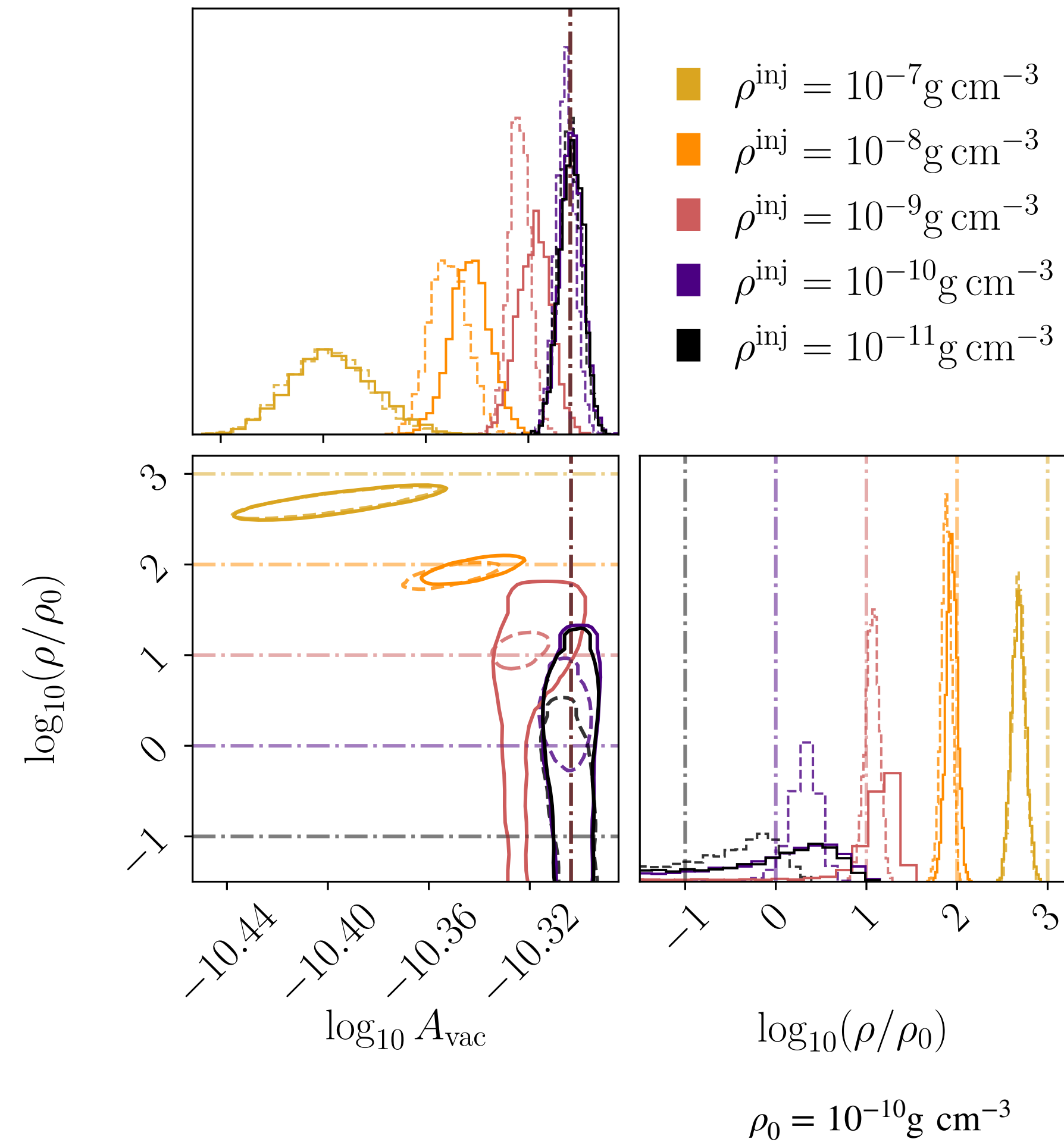
SGWB of sBBH with gas accretion effects in LISA: qualitative detectability



- Vacuum case is above both PLS and BPLS curves in a significant part of the LISA band → vacuum signal potentially detectable
- Gas accretion effects are potentially not detectable due to turning point outside sensitive part of LISA band

Detection and parameter estimation of dynamical friction from SGWB in LISA

We developed parametric models for the SGWB that can be mapped to different environmental effects.
Fully Bayesian data analysis with BAHAMAS [Pozzoli et.al (2025)]



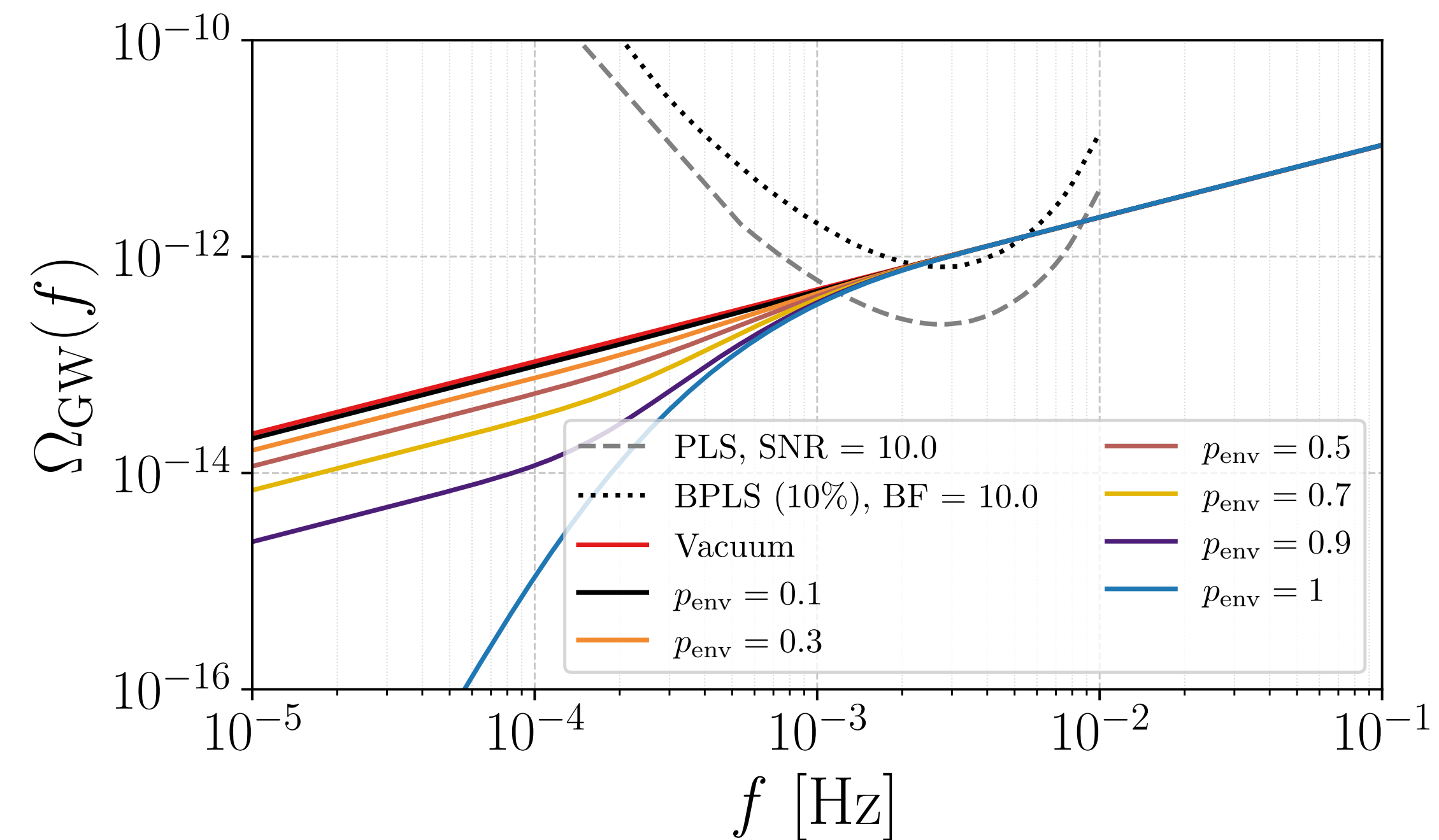
ρ^{inj}/ρ_0	$\delta\rho/\rho^{\text{inj}}$		$\delta A_{\text{vac}}/A_{\text{vac}}^{\text{inj}}$		$\log_{10} \mathcal{B}_{\text{vac}}^{\text{non-vac}}$	
	With	Without	With	Without	With	Without
10^{-1}	37.85	8.218	0.02188	0.01727	1.424	1.010
1	4.248	1.4670	0.02075	0.01490	1.146	3.965
10	1.118	0.4042	0.02114	0.01430	1.777	8.240
10^2	0.3362	0.2033	0.03404	0.02478	1.281	10.16
10^3	0.1606	0.1340	0.05334	0.0493	1.427	7.570

Dynamical friction effects are measurable
and can be distinguished from vacuum

Detecting dynamical friction from a sub-population of sBBH

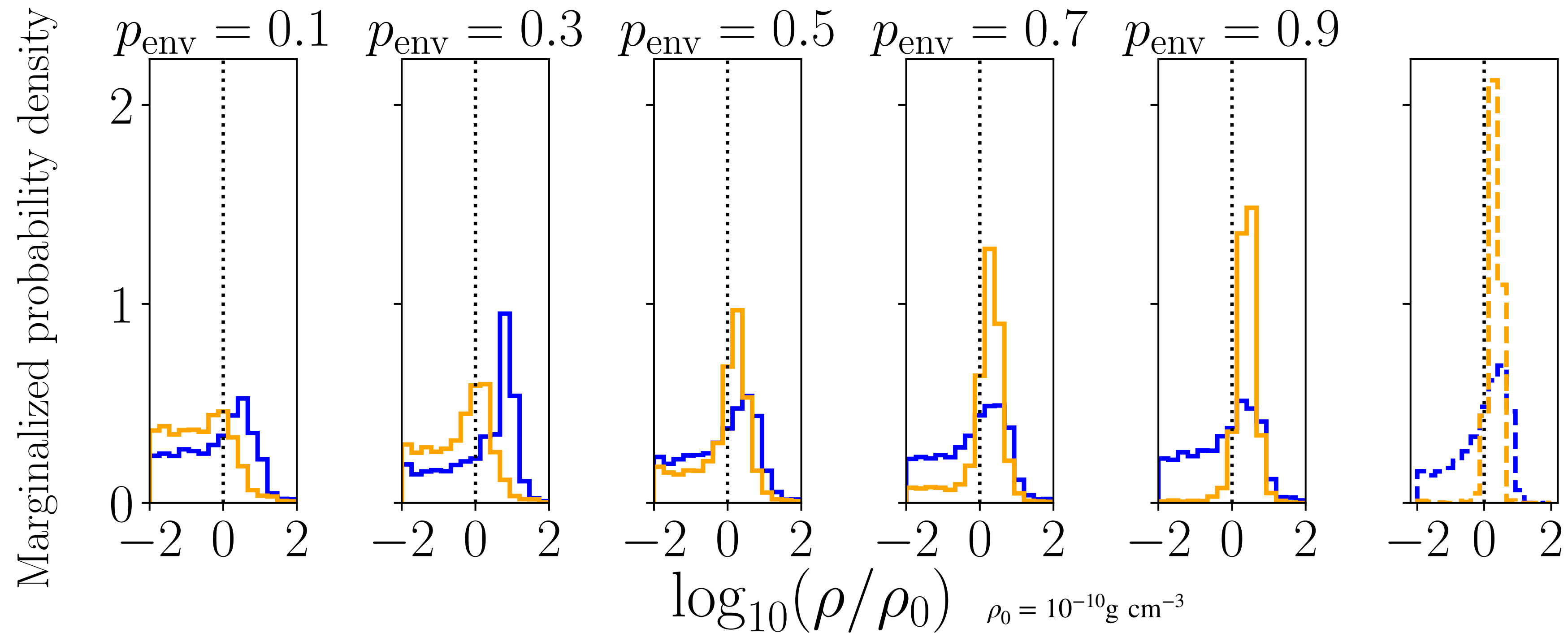
Mixture model to capture sub-population dependence:

$$\Omega_{\text{Frac}} = p_{\text{env}}\Omega_{\text{env}} + (1 - p_{\text{env}})\Omega_{\text{vacuum}}$$



Detecting dynamical friction from a sub-population of sBBH

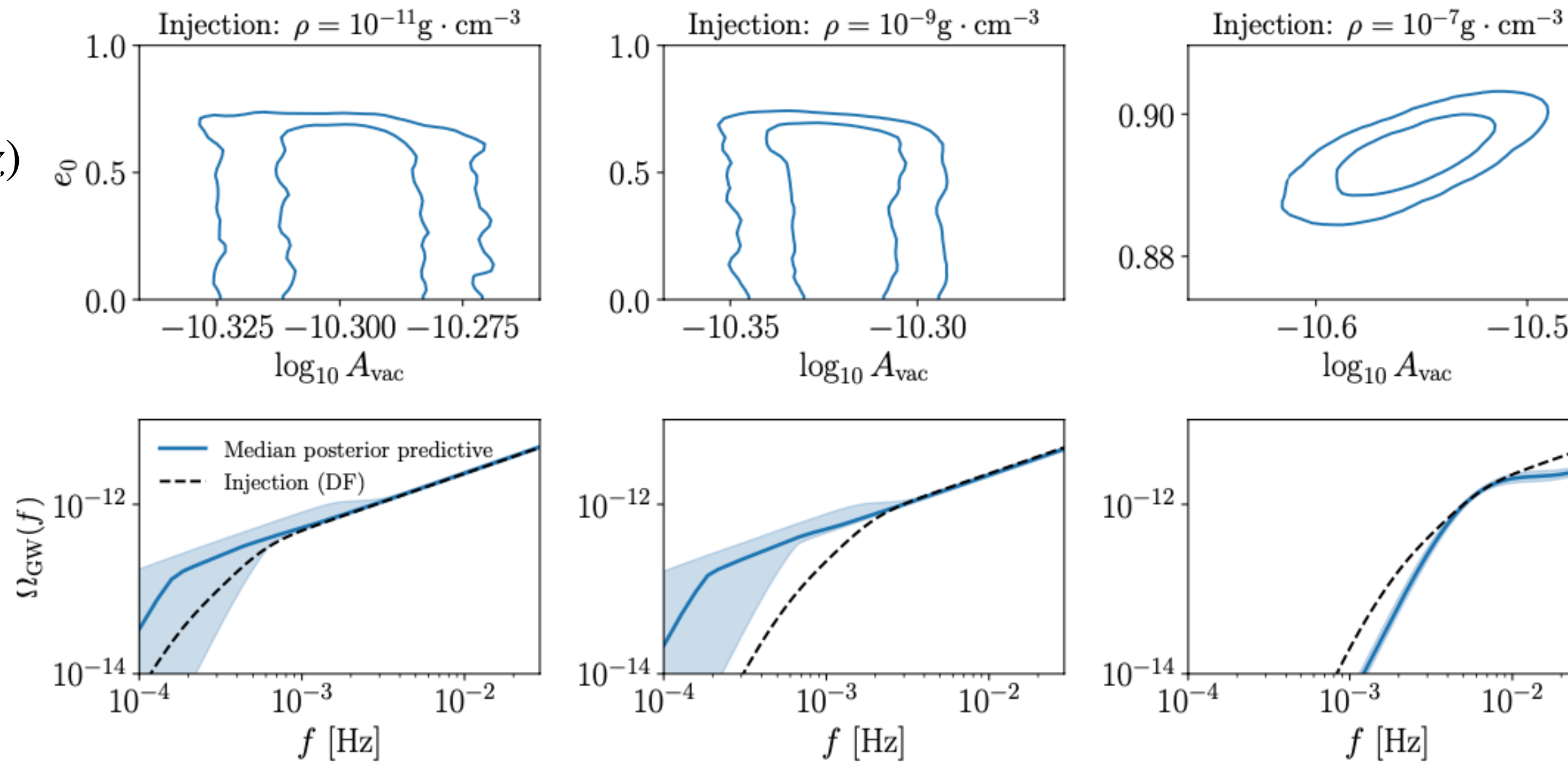
With Galactic foreground (blue histograms): $\log_{10} \mathcal{B}_{\text{vac}}^{\text{Frac}} \sim 0.79 - 0.95$



Substantial preference for mixed fraction model over vacuum—
dynamical friction in sub-populations can be measured

Detecting dynamical friction when allowing for eccentricity in vacuum model

Initial eccentricity
 $e_0 \equiv e(f_{\text{orb},0} = 10^{-4} \text{Hz})$
 follows Dirac-delta
 distribution



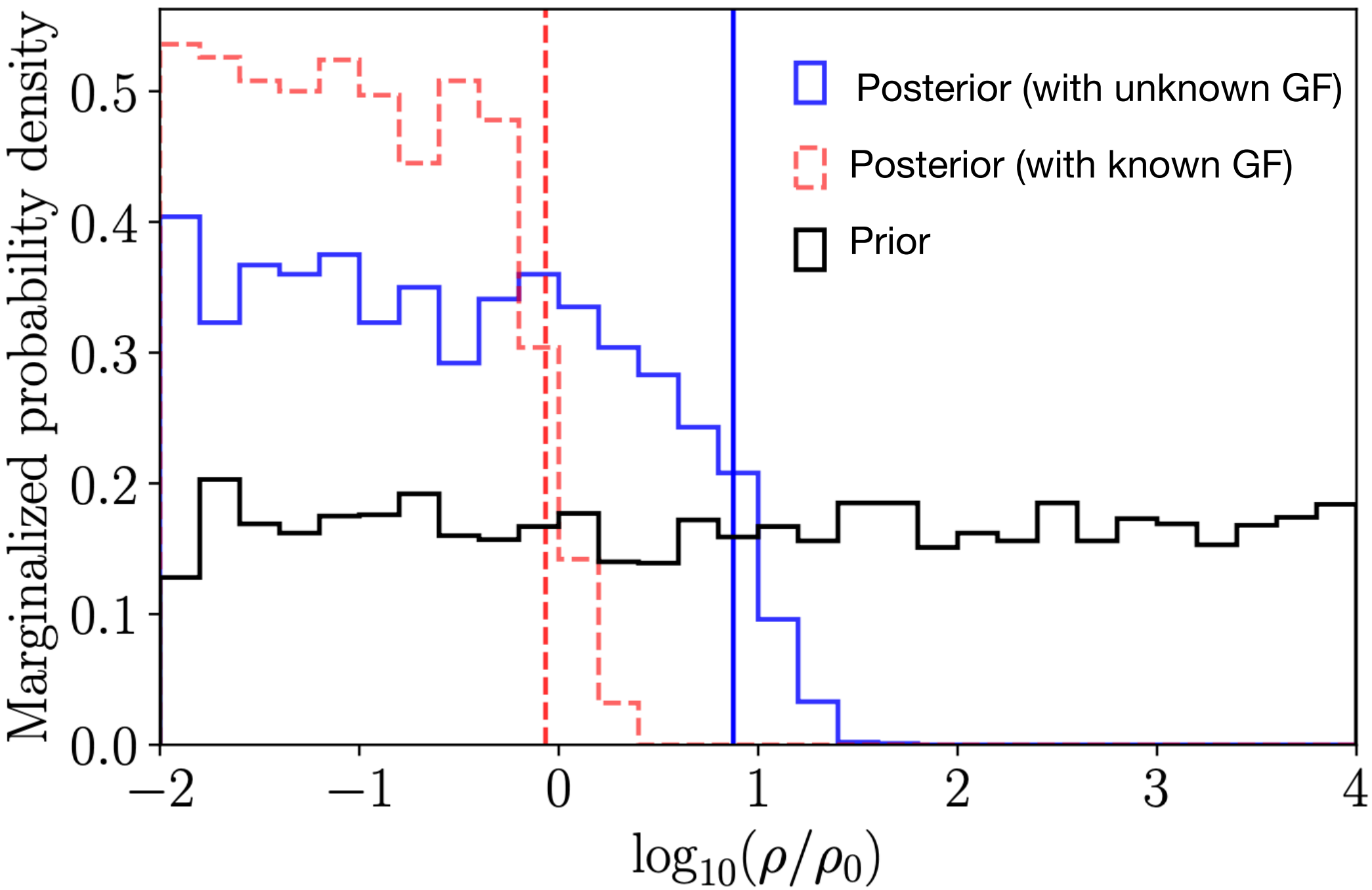
Reconstructed
 posterior predictive
 of the spectrum

ρ (g cm^{-3})	10^{-11}	10^{-10}	10^{-9}	10^{-8}	10^{-7}
$\log_{10} \mathcal{B}_{\text{ecc}}^{\text{DF}}$	-0.01275	0.01033	-0.09733	-0.1328	1.337
$\log_{10} \mathcal{B}_{\text{cir}}^{\text{DF}}$	1.397	1.375	1.407	1.012	1.474

Dynamical friction effects can be distinguished over
 vacuum eccentricity effects for $\rho \gtrsim 10^{-7} \text{gcm}^{-3}$

Constraints on environmental effects

Constraint on disk gas density from detection of vacuum (quasi-circular) SGWB from sBBH:



[Fermi estimate]: More than 10% change compared to quasi circular vacuum prediction above $f \sim 10^{-3} Hz$ when:

Supersonic dynamical friction / Bondi-Hoyle accretion effects (gas / dark matter [-5.5PN]):

$$\rho \gtrsim 10^{-10} \text{gcm}^{-3}$$

Constant mass accretion / CoM acceleration effects [-4PN]:

$$f_{\text{Edd}} \lesssim 10^3 \quad a_{||} \lesssim 10^{-3} \text{m s}^{-2}$$

Takeaways

- For typical gas densities dynamical friction effects can be measured in the LISA stochastic signal. Dynamical friction model is preferred only when $\rho \gtrsim 10^{-7} \text{g cm}^{-3}$ if including eccentricity in the vacuum model.
- For typical Eddington ratios, accretion effects cannot be measured in LISA stochastic signal.
- Improved modeling: “ready-to-use” parametric models for environmental or eccentricity effects in SGWB

Future work

- Interplay of eccentricity and environmental effects in the orbital evolution and stochastic background
 - Improved modeling of environmental effects such as dynamical friction (mutual wake effect, disk profile etc.)
 - Expected distribution of eccentricities (and semi-major axes) under different astrophysical channels and interactions with environment
- Role of extragalactic foreground on the detection of the SGWB from sBBHs

Extra slides

Primer on SGWB from vacuum sBBH: quantitative

[Allen & Romano (2001), Phinney (2001), Abbott et al (2021)]

$$\Omega_{\text{GW}}(f) = \frac{f}{\rho_c H_0} \iint dz d\phi \frac{R_{\text{GW}}(z)}{(1+z)\mathcal{E}(z)} p(\phi) \frac{dE_{\text{GW}}}{df_s}(\phi) \Big|_{f_s=f(1+z)}$$

Comoving merger rate
Source params (masses, spins etc.)

Prob. distribution of source params

$$\frac{dE_{\text{GW}}}{df_s} \equiv \frac{\dot{E}_{\text{GW}}}{\dot{f}_s} = \frac{\eta m^{5/3} \pi^{2/3}}{3f_s^{1/3}}$$

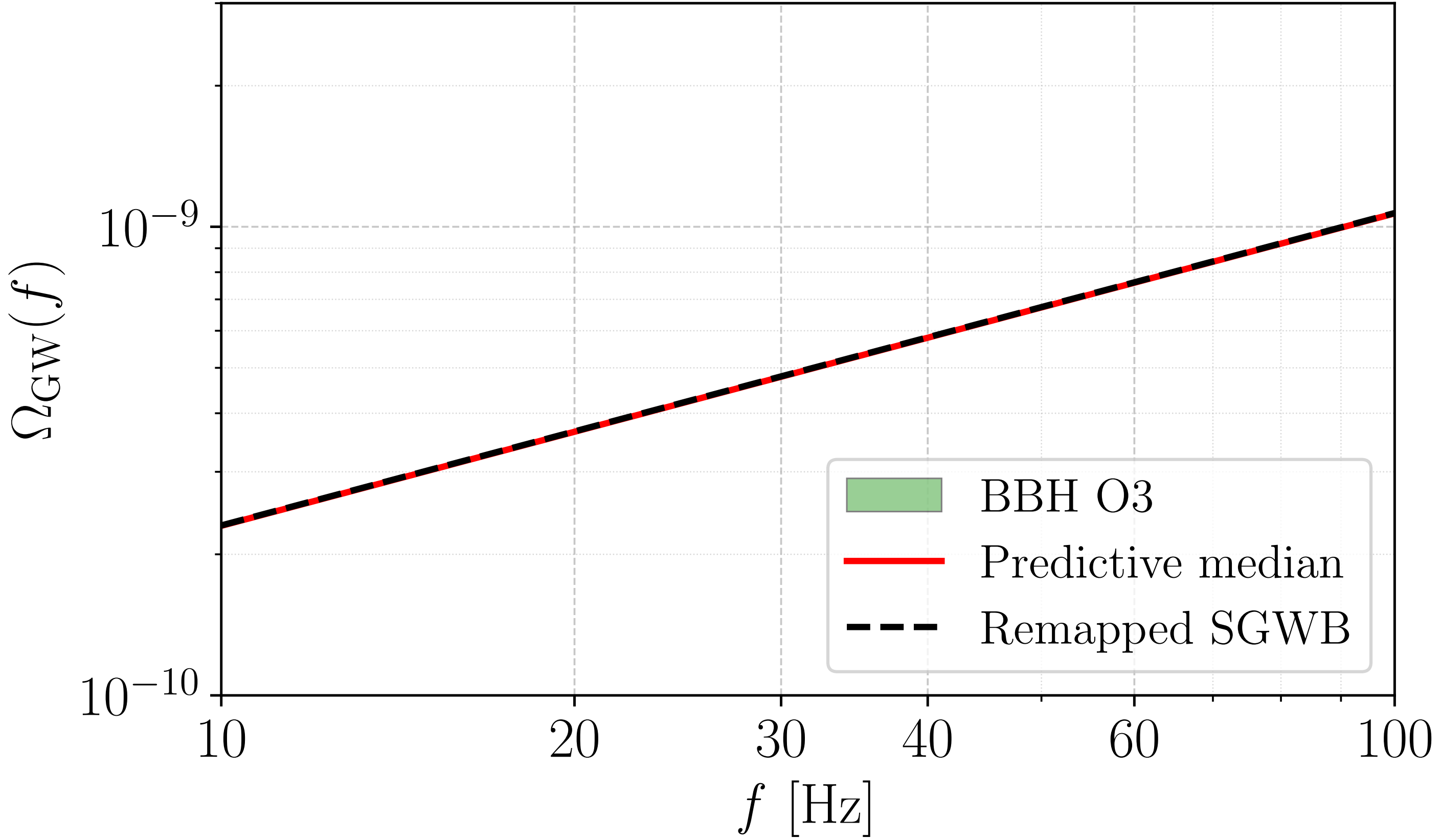
GW energy flux

$$\Omega_{\text{GW}}(f) = A_{\text{vac}} f^{2/3}$$

$$A_{\text{vac}} = \frac{\pi^{2/3}}{3\rho_c H_0} \iiint dm_1 dq dz \frac{R_{\text{GW}}(z) p(m_1, q)}{(1+z)^{4/3} \mathcal{E}(z)} \eta m^{5/3} \approx 4.97 \times 10^{-11} [\text{Hz}^{-2/3}]$$

Median amplitude informed by LVK constraints on merger rate and mass distribution

SGWB from unresolved (vacuum) sBBH in LVK band



Improved model for eccentric SGWB

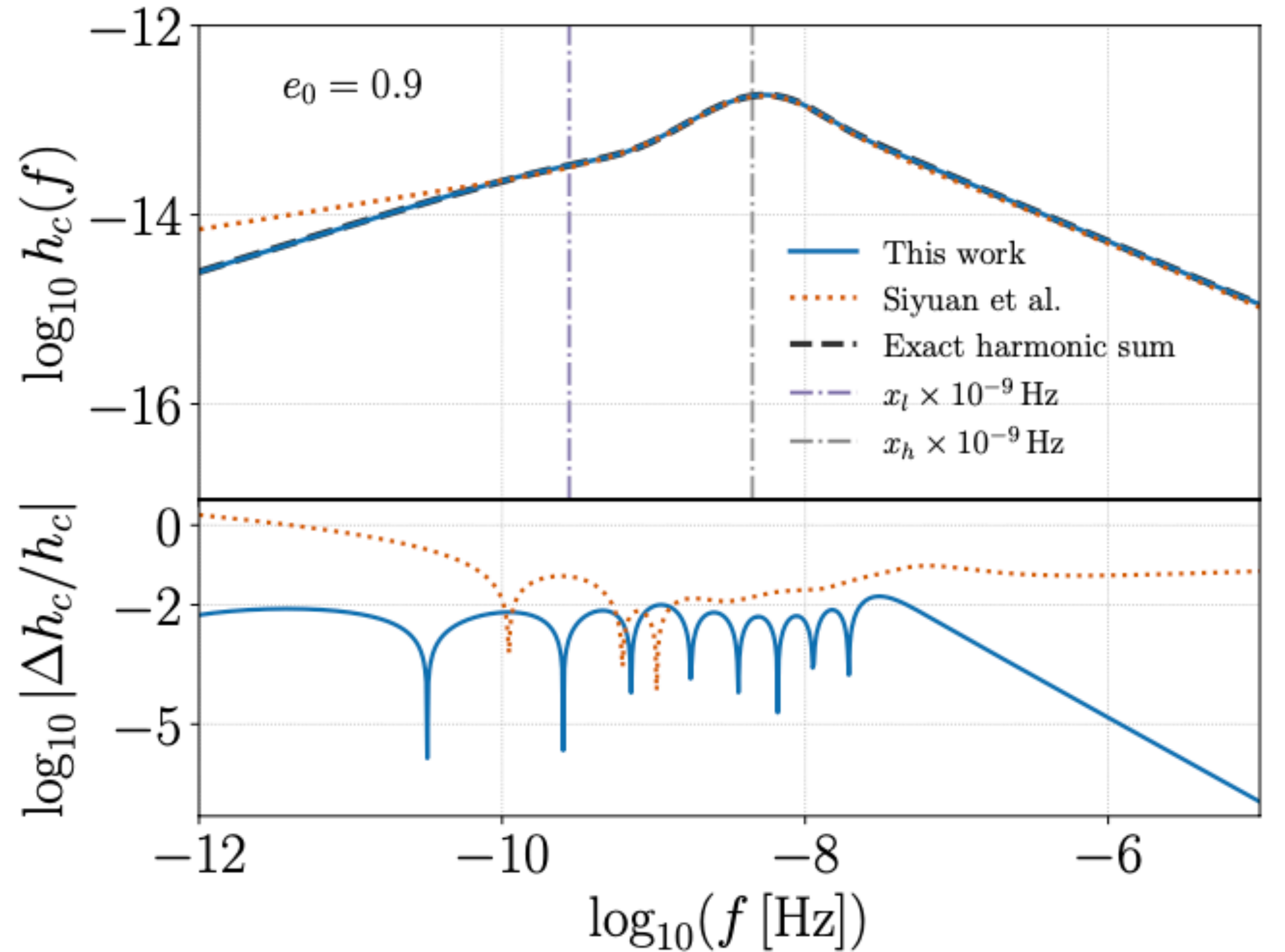
$$h_{c,\text{fit}}^2(x) = h_{c,\text{circ}}^2(x) S_{\text{fit}}(x), \quad (20a)$$

$$S_{\text{fit}}(x) = \frac{(x/x_a)^{q_a}}{1 + (x/x_a)^{q_a}} \times \left[1 + A_l \left(\frac{x}{x_l} \right)^{p_l} \exp(-x/x_l) \right] \times \left[1 + A_h \left(\frac{x}{x_h} \right)^{p_h} \exp(-x/x_h) \right], \quad (20b)$$

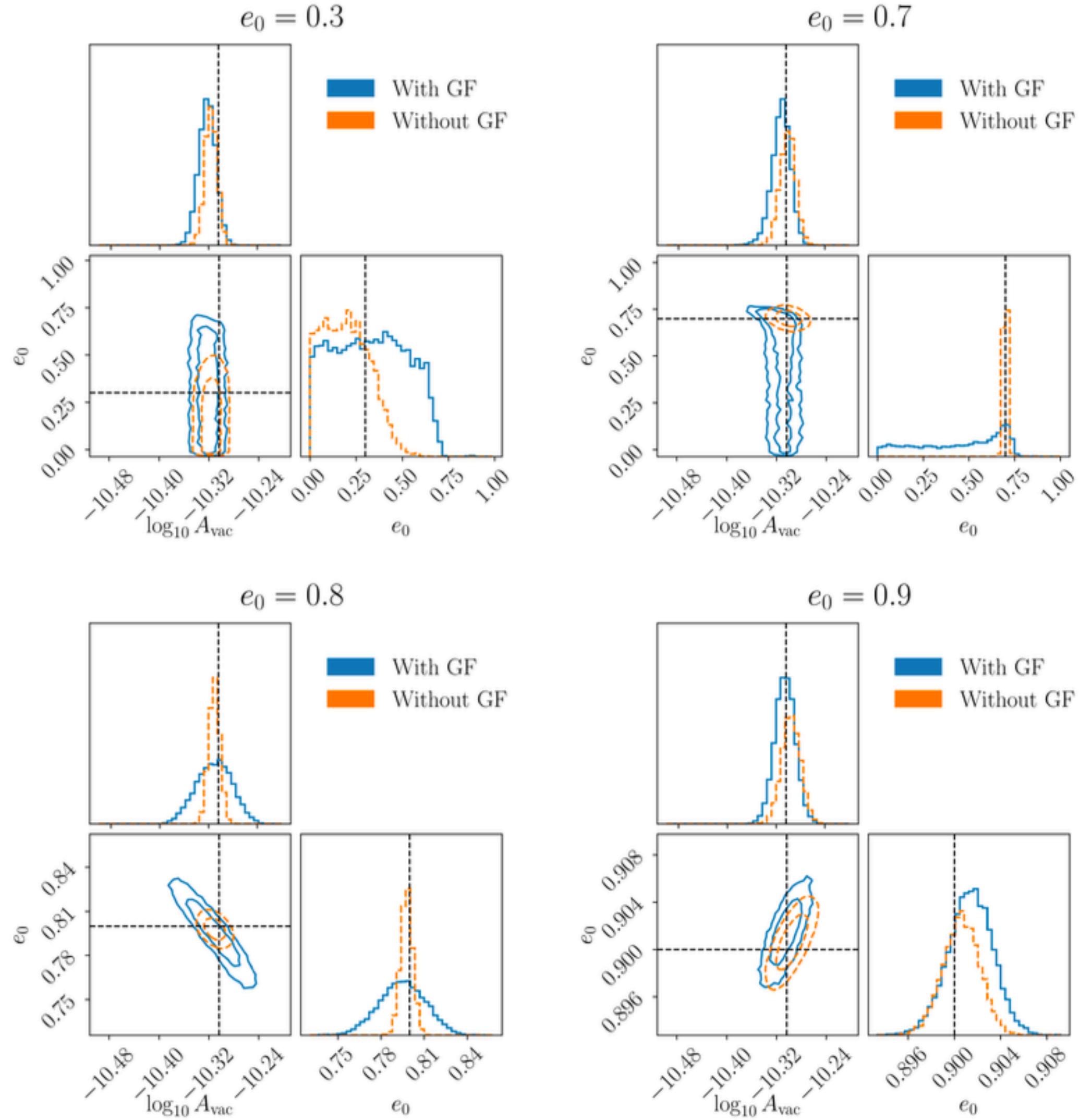
$$h_c^2(f) = A_{\text{pop}} \times h_{c,\text{fit}}^2 \left(f \frac{f_{p,\text{ref}}}{f_p} \right) \left(\frac{f_p}{f_{p,\text{ref}}} \right)^{-4/3}, \quad (24)$$

with the dimensionless amplitude A_{pop} given by

$$A_{\text{pop}} = \int dz dm_1 dq \frac{R_{\text{GW}}(z) p(m_1, q)}{H_0 \mathcal{E}(z) (1+z) \text{Mpc}^{-3}} \times \left(\frac{\mathcal{M}}{\mathcal{M}_0} \right)^{5/3} \left(\frac{1+z}{1+z_0} \right)^{-1/3}. \quad (25)$$



Measuring eccentricity: Dirac delta distribution injection-recovery



e_0^{inj}	$e_{f_{\text{orb}}=10 \text{ Hz}}$	SNR	$\delta e_0 / e_0^{\text{inj}}$	$\delta A_{\text{vac}} / A_{\text{vac}}^{\text{inj}}$	$\log_{10} \mathcal{B}_{\text{cir}}^{\text{ecc}}$
0.1	5.372×10^{-7}	200	3.069	0.05113	0.7360
0.2	1.136×10^{-6}	200	1.557	0.05049	0.9060
0.3	1.877×10^{-6}	200	0.9955	0.05064	0.6035
0.4	2.886×10^{-6}	201	0.7568	0.05172	0.7175
0.5	4.402×10^{-6}	201	0.6461	0.05049	0.8518
0.6	6.952×10^{-6}	206	0.5232	0.05081	0.9513
0.7	1.193×10^{-5}	228	0.4814	0.05650	0.8157
0.8	2.437×10^{-5}	282	0.03269	0.1073	0.2662
0.9	7.783×10^{-5}	181	0.003499	0.06279	11.12

Energy spectrum of eccentric binaries

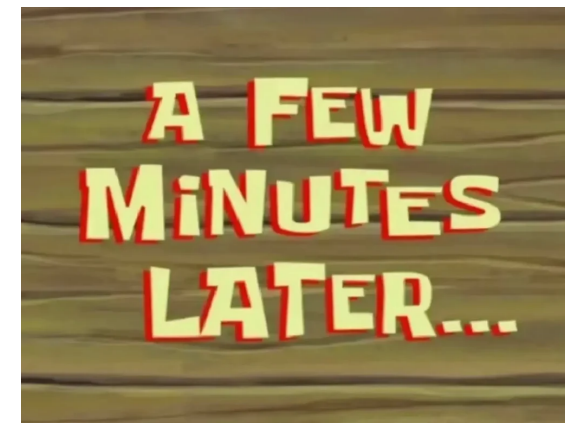
Waveform in frequency domain (stationary phase approximation)

$$\tilde{h}_{+, \times} = -\frac{\eta m}{2D_L} \sum_{j=1}^{\infty} \frac{[2\pi m f_{\text{orb}}(t_j^*)]^{2/3}}{\sqrt{j \dot{f}_{\text{orb}}(t_j^*)}} \times \left[C_{+, \times}^{(j)}(t_j^*) + i S_{+, \times}^{(j)}(t_j^*) \right] e^{-i\psi_j(t_j^*)},$$

For expressions of mode amplitudes that do not contain typos, refer to [\[RSC & Yunes \(2022\)\]](#)

Relation between energy spectrum and polarizations [\[Phinney \(2001\)\]](#)

$$\frac{dE_{\text{GW}}}{df_r} = 2\pi^2 \frac{D_L^2}{(1+z)^2} f^2 \times \left(\langle |\tilde{h}_+(f_r)|^2 \rangle + \langle |\tilde{h}_\times(f_r)|^2 \rangle \right) \Big|_{f_r=f(1+z)},$$



$$\frac{dE_{\text{GW}}}{df_r} = \frac{\mathcal{M}^{5/3} \pi^{2/3}}{3f^{1/3} (1+z)^{1/3}} \sum_{j=1}^{\infty} \frac{g(j, e_j)}{F(e_j) (j/2)^{2/3}}$$

See [\[Enoki & Nagashima \(2007\)\]](#) for a different derivation

Primer on eccentric binaries

- Multi-periodic (epicyclic) orbital motion

$$r = a(1 - e \cos u)$$

$$\tan(v/2) = \sqrt{\frac{1+e}{1-e}} \tan(u/2)$$

$$l = n(t - t_p) = u - e \sin(u) \quad \text{Kepler equation}$$

[Yunes et.al (2008)]

$$\cos \phi = -e + \frac{2}{e}(1 - e^2) \sum_{k=1}^{\infty} J_k(ke) \cos kl, \quad (2.13)$$

$$\sin \phi = (1 - e^2)^{1/2} \sum_{k=1}^{\infty} [J_{k-1}(ke) - J_{k+1}(ke)] \sin kl. \quad (2.14)$$

- GW Radiation reaction \rightarrow loss of energy and angular momentum \rightarrow shrinking and circularizing of orbit

$$\left\langle \frac{da}{dt} \right\rangle = -\frac{64}{5} \frac{G^3 m_1 m_2 (m_1 + m_2)}{c^5 a^3 (1 - e^2)^{7/2}} \left(1 + \frac{73}{24} e^2 + \frac{37}{96} e^4 \right)$$

[Peters (1964)]

$$\left\langle \frac{de}{dt} \right\rangle = -\frac{304}{15} \frac{G^3 m_1 m_2 (m_1 + m_2)}{c^5 a^4 (1 - e^2)^{5/2}} \left(1 + \frac{121}{304} e^2 \right).$$

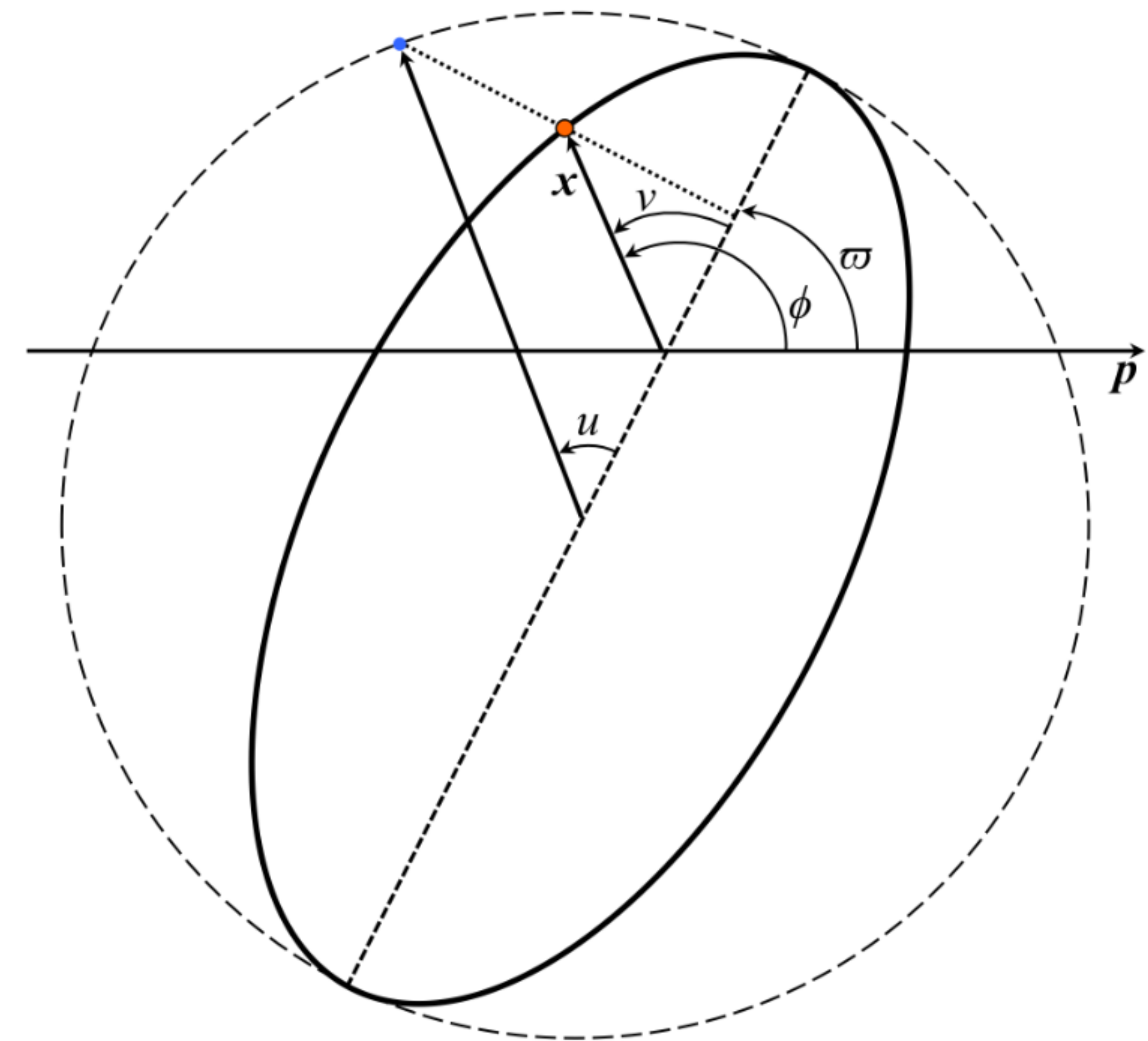


Figure adapted from Moore et al (2016)

Bayesian parameter estimation of SGWB in LISA

$$\ln \mathcal{L}(\hat{\mathbf{S}} \mid \theta) = \sum_{i=1}^D \sum_k \left[-\ln \Gamma(N) - N \ln \left(\frac{S_k(f_i; \theta)}{N} \right) + (N-1) \ln \hat{S}_k(f_i) - \frac{N \hat{S}_k(f_i)}{S_k(f_i; \theta)} \right],$$

$$S_{k,\text{GW}}(f; \theta) = R_k(f; \theta) S_{\text{GW}}(f; \theta) \quad S_{\text{GW}}(f; \theta) = \frac{3H_0^2}{4\pi^2 f^3} \Omega_{\text{GW}}(f; \theta)$$

$$S_{\text{GW,Gal}}(f; \theta_{\text{Gal}}) = \frac{A_{\text{Gal}}}{2} f^{-7/3} \exp \left[- (f/f_1)^{\alpha_{\text{Gal}}} \right] \left[1 + \tanh((f_{\text{kn}} - f)/f_2) \right]$$

$$\text{SNR} = \sqrt{T \sum_k 4 \int_0^\infty df \left(\frac{S_{k,\text{GW}}(f)}{S_{k,n}(f)} \right)^2}$$

Phenomenological parametric models for environmental effects in SGWB

For “ready-to-use” in parameter estimation, we developed new phenomenological parametric models of the SGWB that can be mapped to different environmental effects

Rational power law model:
$$\Omega_{\text{RPL}} = \frac{A_{\text{vac}} f^\gamma}{1 + A_m \alpha f^\beta [\ln(f/1\text{Hz})]^\kappa}$$

Captures the SGWB at both low and high frequencies. Coefficients and spectral indices determined from asymptotic matching

Rational power law + peak model:
$$\Omega_{\text{RPLP}} = \frac{\Omega_{\text{RPL}}}{1 + \mathcal{G}(f, \alpha)} \rightarrow$$
 Gaussian “peak” correction to fit better at intermediate frequencies

Parameter	Dynamic Friction	Accretion
α	ρ	$(5 + 3\xi) f_{\text{Edd}}/\tau$
β	$-11/3$	$-8/3$
κ	1	0
<i>Asymptotic matching parameters</i>		
A_{vac}	4.97×10^{-11}	4.97×10^{-11}
A_m	-2.73×10^{-7}	4.35×10^2
<i>Gaussian spectral correction parameters</i>		
A_g	$1.02 - 0.0262 \log_{10}(\alpha/\alpha_0)$	0.904
f_{peak}	$0.0269 (\alpha/\alpha_0)^{0.262}$	$9.73 (\alpha/\alpha_0)^{0.374}$
σ	0.222	0.321

Bayesian parameter estimation of LISA SGWB

Coarse-grained likelihood [Appourchaux (2003)] implemented in BAHAMAS [Pozzoli et al (2025)]:

$$\ln \mathcal{L}(\hat{\mathcal{S}} \mid \theta) = \sum_{i=1}^D \sum_k \left[-\ln \Gamma(N) - N \ln \left(\frac{S_k(f_i; \theta)}{N} \right) + (N-1) \ln \hat{S}_k(f_i) - \frac{N \hat{S}_k(f_i)}{S_k(f_i; \theta)} \right],$$

$$S_k(f; \theta) = S_{\text{GW}}(f; \theta) + S_{k,n}(f; \theta),$$

PSD of
channel k

SGWB PSD

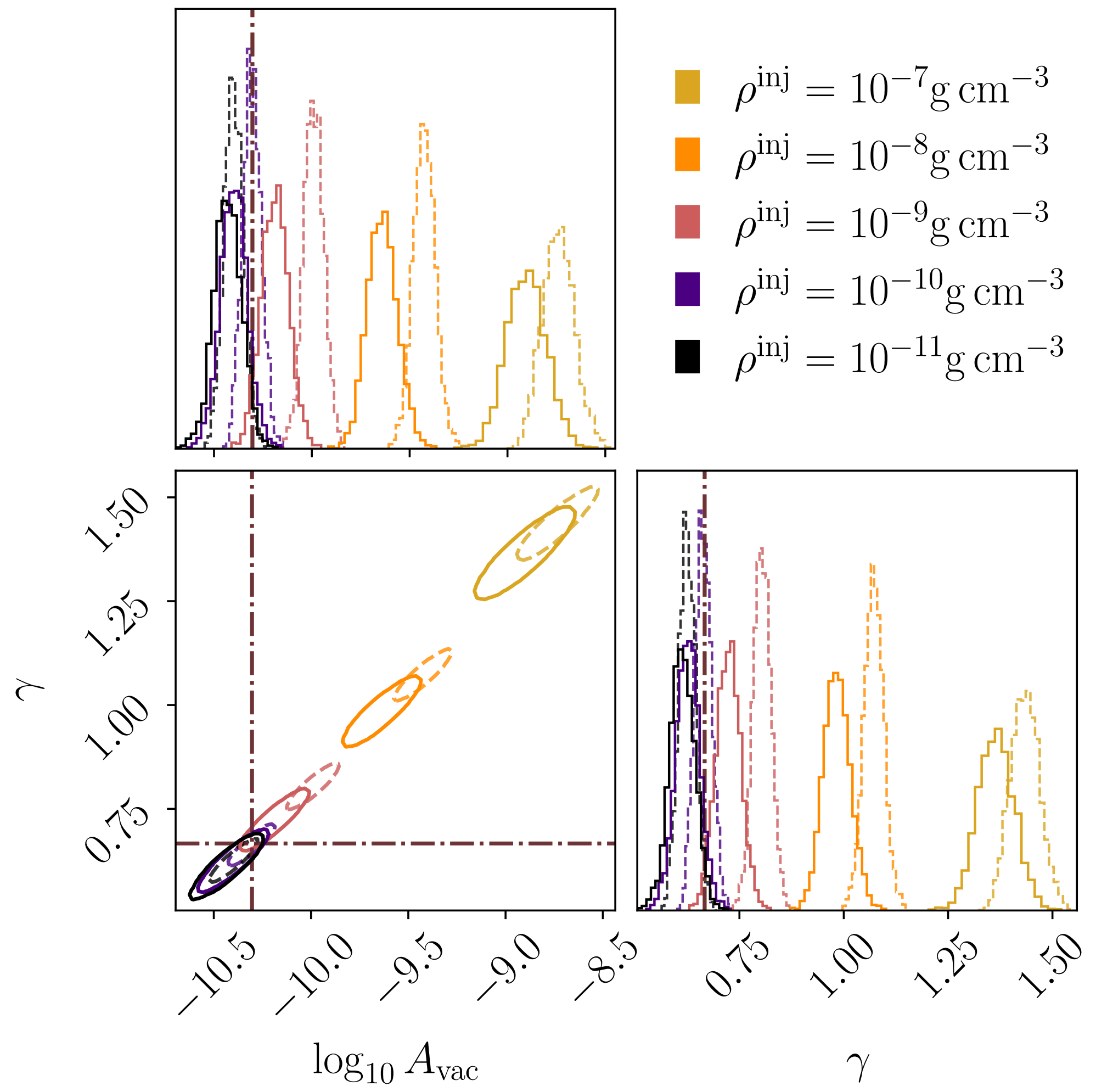
Instrumental PSD

LISA response
for channel k

PSD of astrophysical SGWB
(both from sBBH and GB)

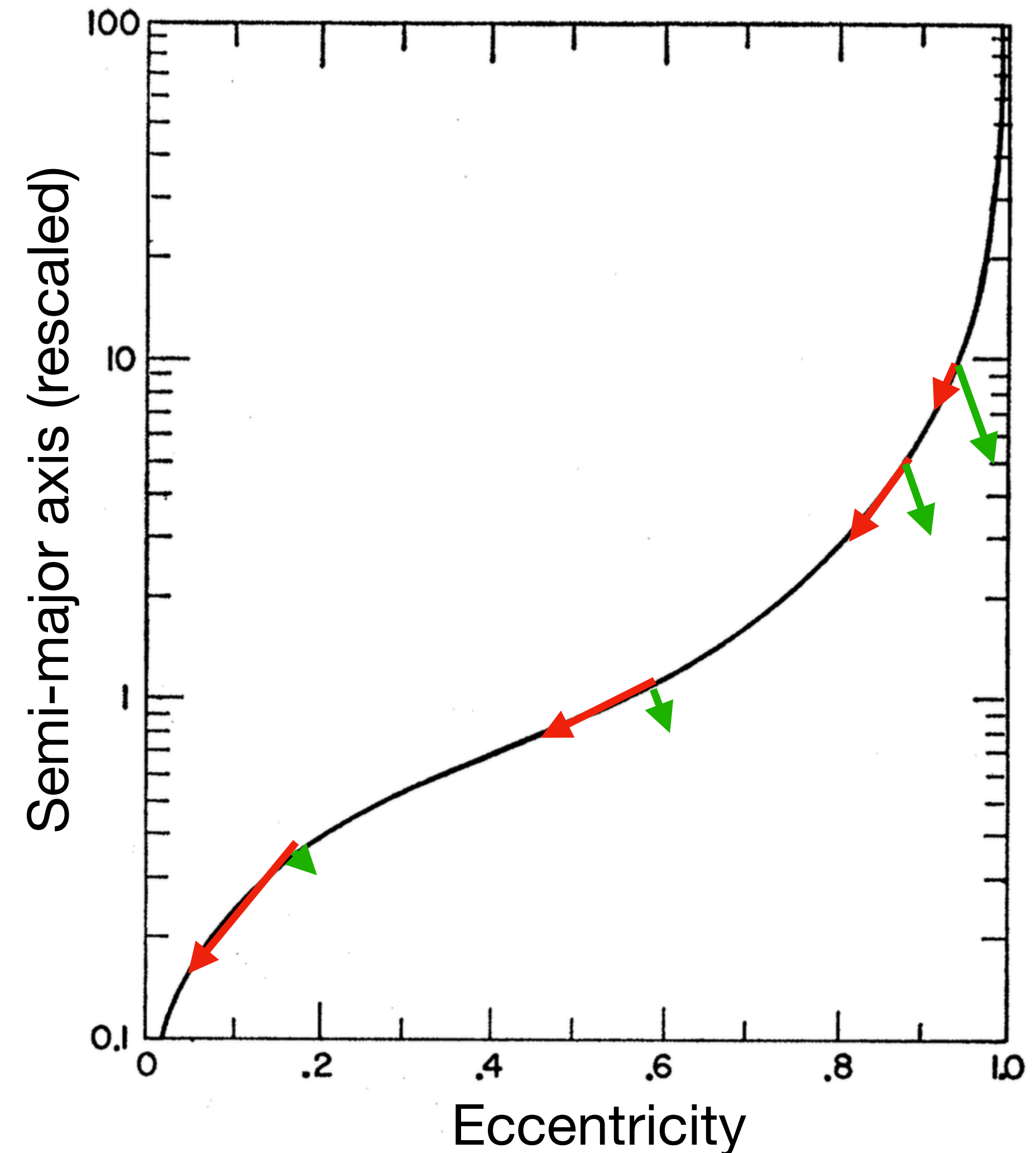
$$S_{k,\text{GW}}(f; \theta) = R_k(f; \theta) S_{\text{GW}}(f; \theta), \quad S_{\text{GW}}(f; \theta) = \frac{3H_0^2}{4\pi^2 f^3} \Omega_{\text{GW}}(f; \theta)$$

Systematic biases due to neglecting dynamical friction



Early inspiral, low frequency regime of stellar mass black hole binaries: window into eccentricity

- In vacuum, GW radiation reaction leads to shrinking and circularizing of orbits [Peters (1964)]
- In an astrophysical environment, eccentricity can be excited due to gas and third body torques: potentially compete with GW radiation reaction [Gair et.al (2011), Rodig et.al (2011), Cardoso et.al (2021), RSC & Yunes (2022), Duque et.al (2024)]
- Thus, early inspiral probes eccentricity potentially caused by astrophysical environment



[adapted from Peters (1964)]

Primer on gravitational waves from eccentric binaries

GW signal is thus a sum of harmonics

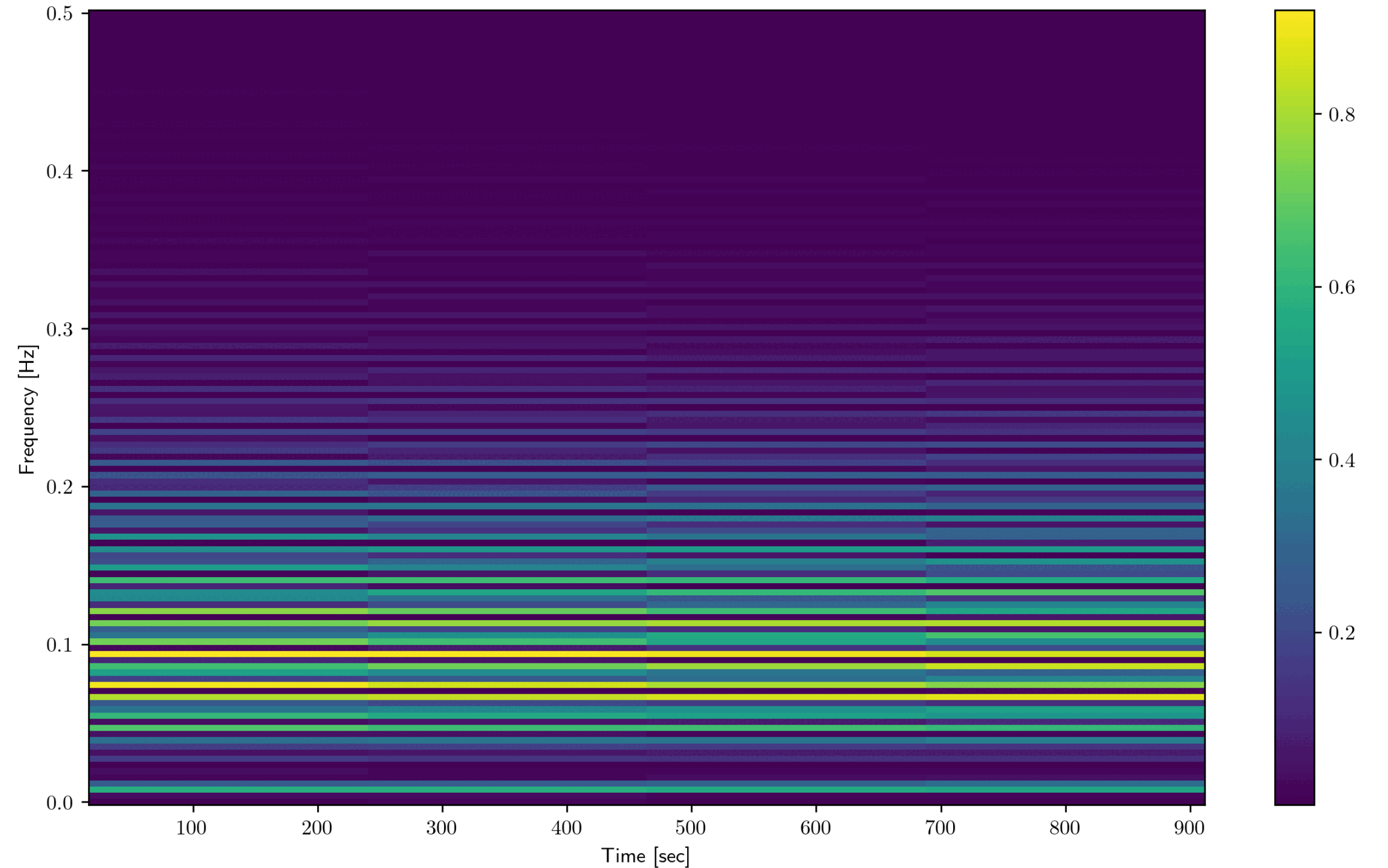
$$h_{+, \times}(t) = -\frac{m\eta}{R} (2\pi m F)^{2/3} \sum_{j=1}^{\infty} \left[C_{+, \times}^{(j)} \cos jl + S_{+, \times}^{(j)} \sin jl \right] \quad [\text{Moore et al (2018)}]$$

Power emitted into each harmonic:

$$P_{\text{GW}, j} \equiv \frac{dE_{\text{GW}, j}}{dt} = \frac{32}{5} (2\pi f_{\text{orb}} \mathcal{M})^{10/3} g(j, e_j),$$

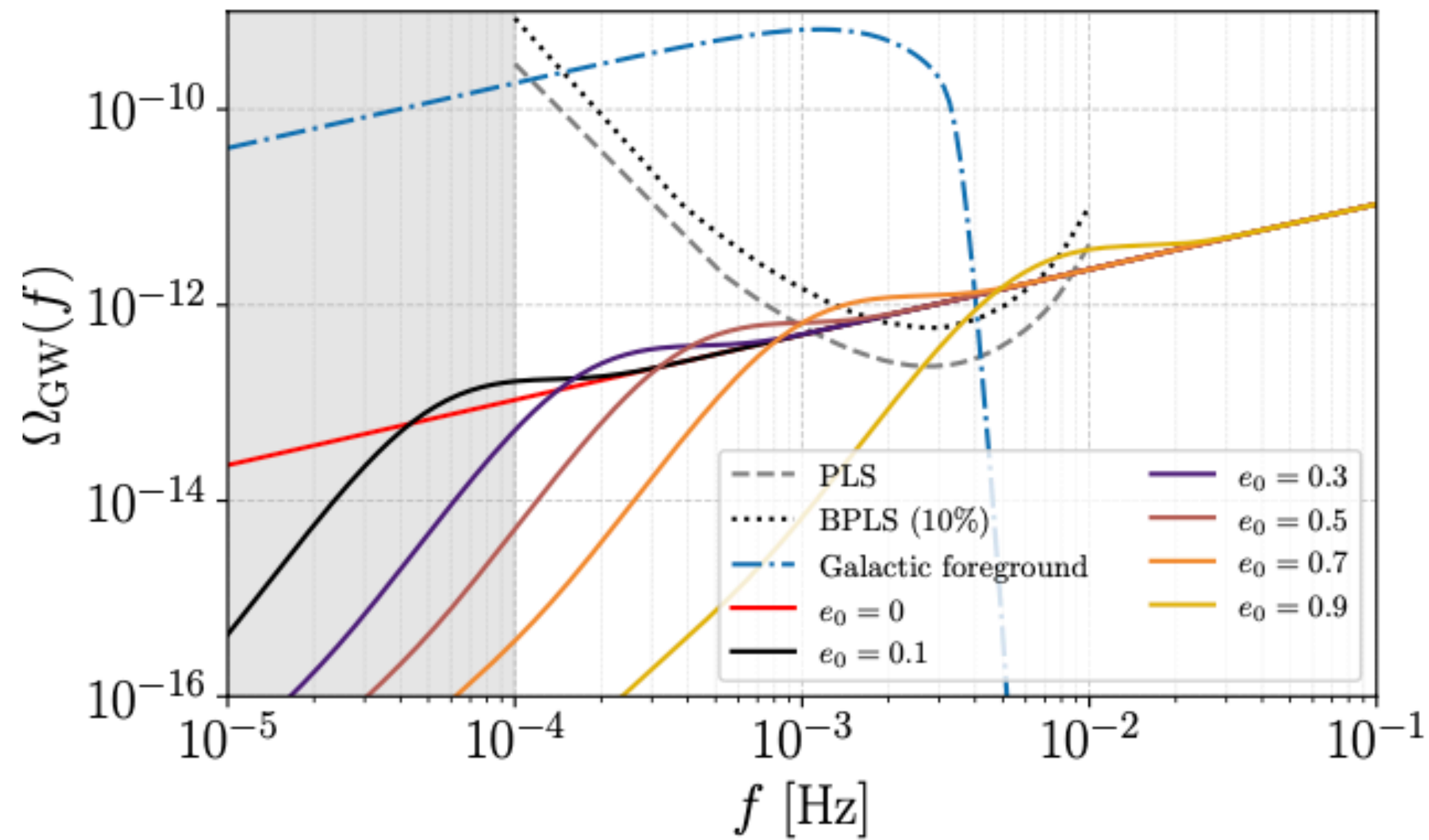
[Peters & Mathews (1963)]

$$g(j, e) = \frac{j^4}{32} \left[\left\{ J_{j-2}(je) - 2eJ_{j-1}(je) + \frac{2}{j} J_j(je) + 2eJ_{j+1}(je) - J_{j+2}(je) \right\}^2 + (1 - e^2) \left\{ J_{j-2}(je) - 2J_j(je) + J_{j+2}(je) \right\}^2 + \frac{4}{3j^2} J_j^2(je) \right].$$



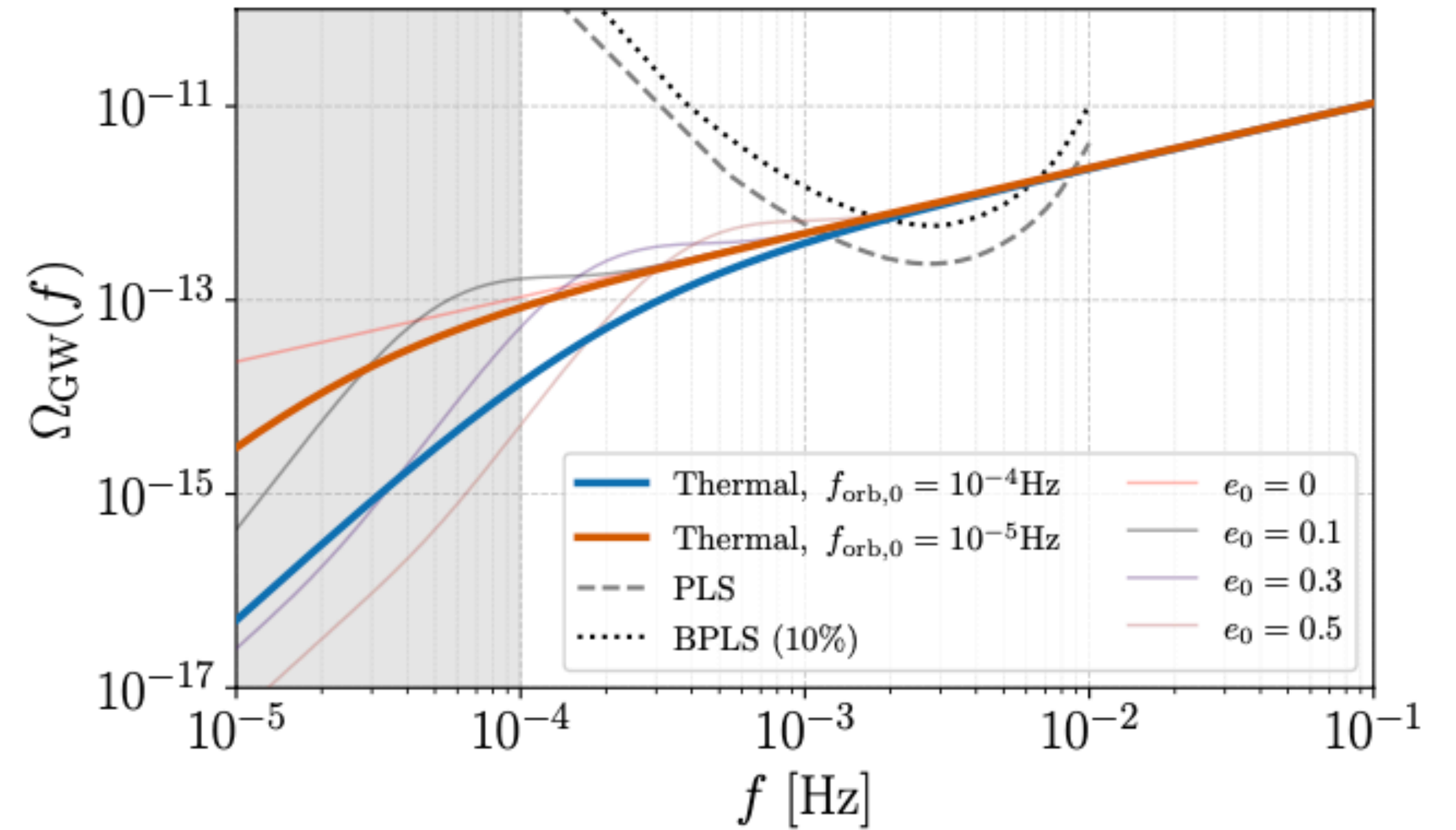
Signatures of eccentricity in LISA band

Dirac delta distribution



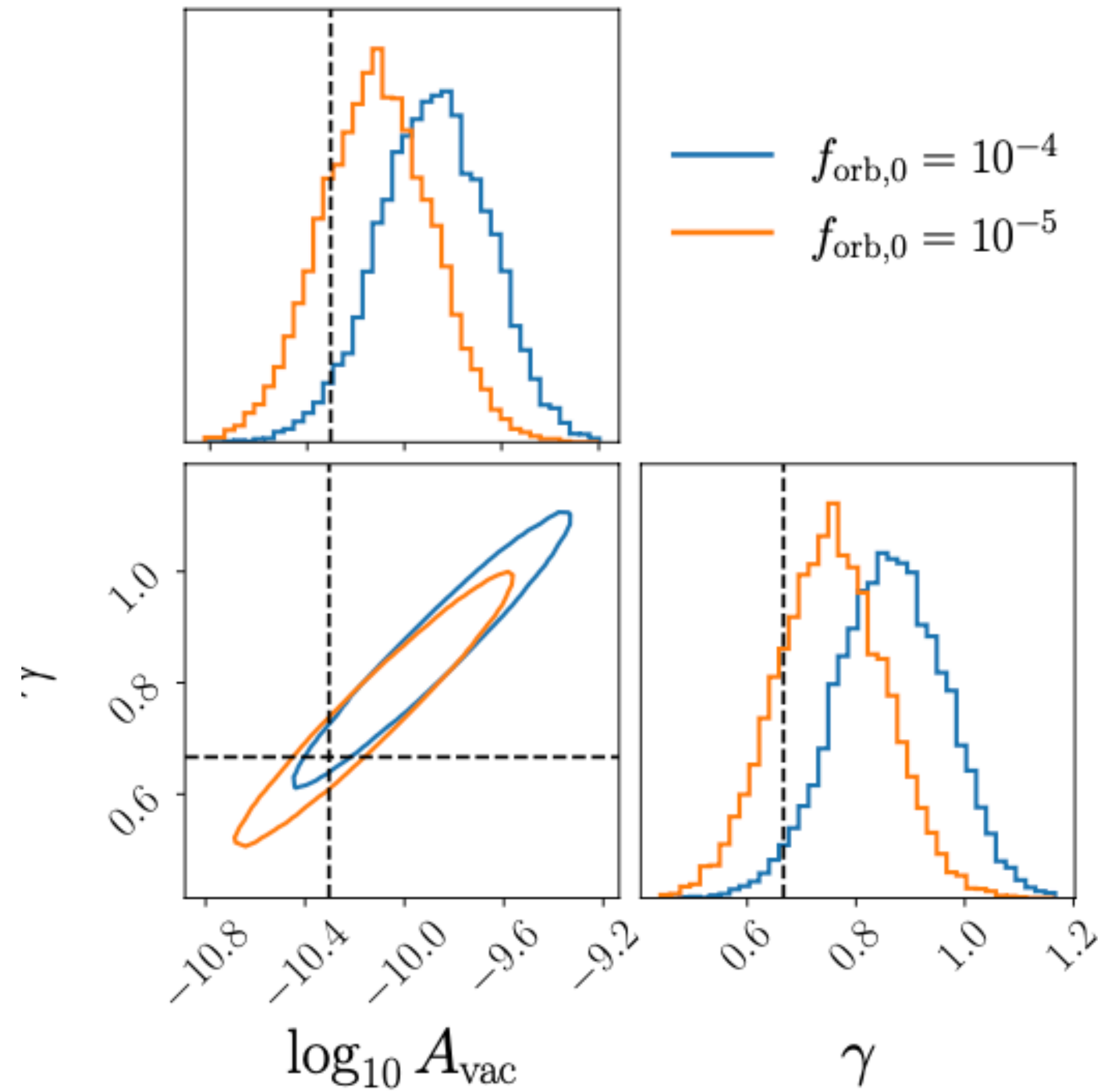
Initial eccentricity $e_0 \equiv e(f_{\text{orb},0} = 10^{-4} \text{ Hz})$

Thermal distribution



Initial eccentricity $e_0 \equiv e(f_{\text{orb},0})$ follows $p(e_0) \sim 2e_0$

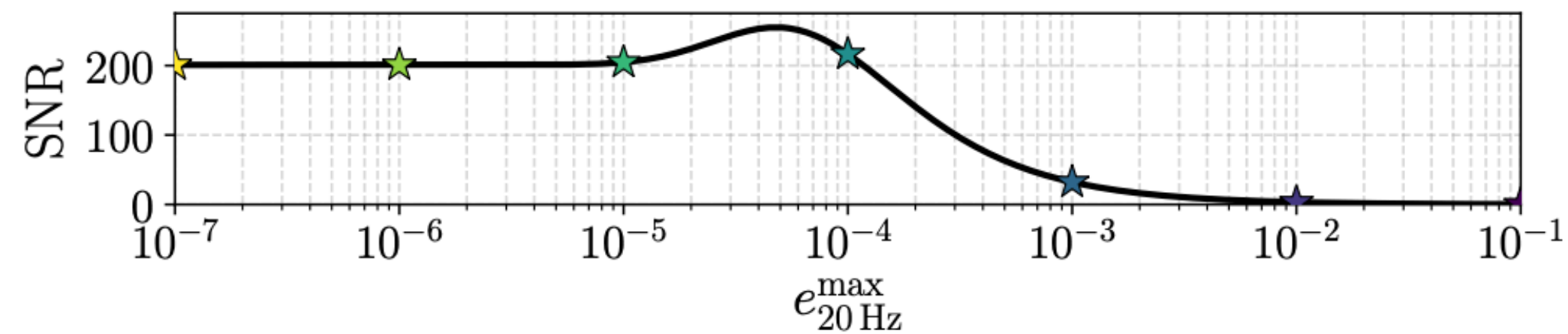
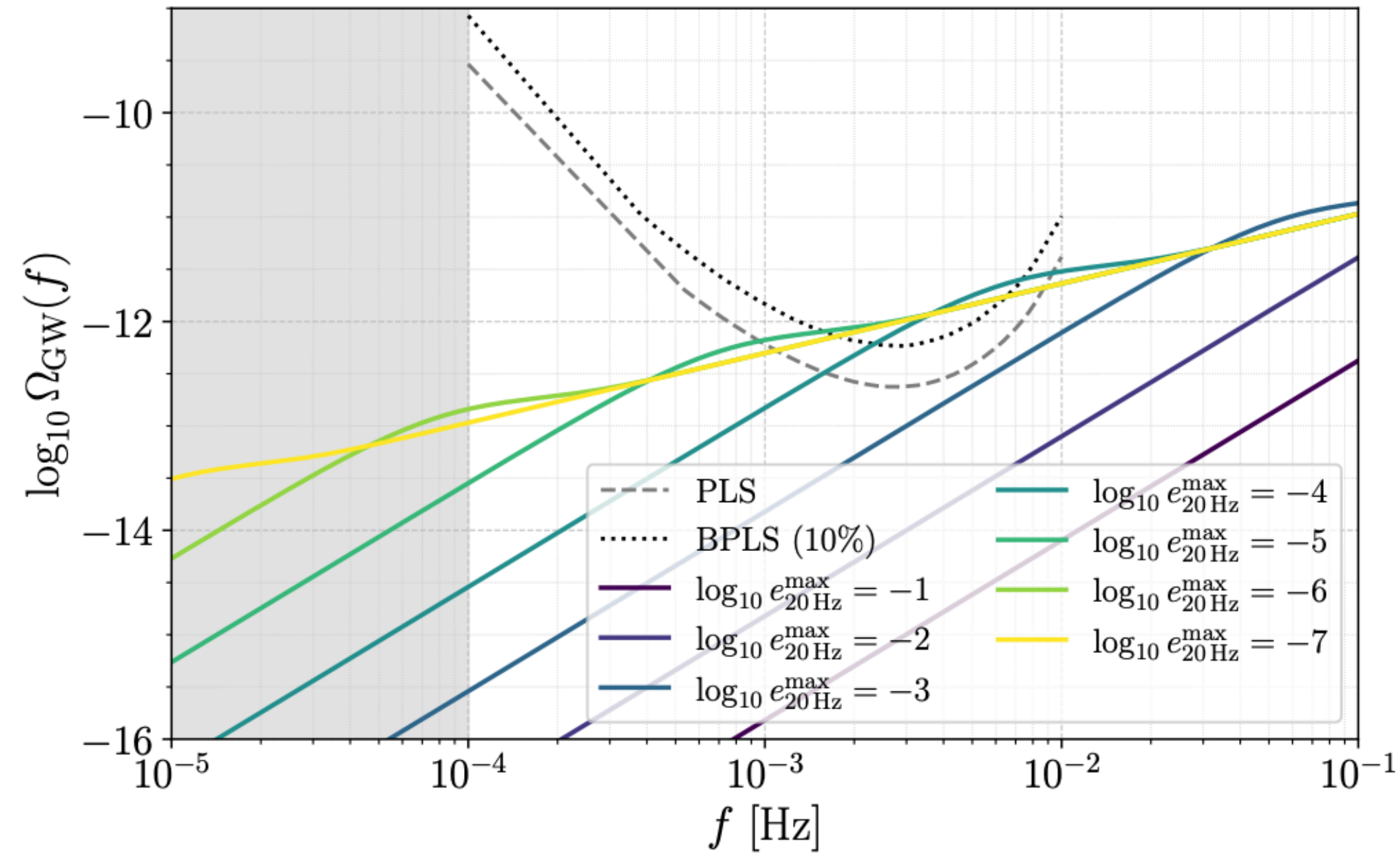
Bias in circular model parameters: thermal distribution injection



Bias in circular model parameters increases with $f_{\text{orb},0}$

Constraining eccentricity in LVK band through non-detection of SGWB in LISA band

Eccentricity $e(f_{(2,2)} = 20\text{Hz}) \sim U(0, e_{20\text{Hz}}^{\max})$



For $e_{20\text{Hz}}^{\max} \gtrsim 10^{-2} \rightarrow \text{SNR} \lesssim 3$ and thus the signal will be difficult to detect

Detection and parameter estimation of gas accretion from SGWB in LISA

Gas accretion effects cannot be measured even for large Eddington ratio (Bayesian analysis)

